



# **NAVAL POSTGRADUATE SCHOOL**

**MONTEREY, CALIFORNIA**

## **THESIS**

**PERFORMANCE ANALYSIS OF AN ALTERNATIVE  
LINK-16/JTIDS WAVEFORM TRANSMITTED OVER A  
CHANNEL WITH PULSE-NOISE INTERFERENCE**

by

Cham Kok Kiang

March 2008

Thesis Advisor:  
Second Reader:

Clark Robertson  
Roberto Cristi

**Approved for public release; distribution is unlimited**

THIS PAGE INTENTIONALLY LEFT BLANK

<b>REPORT DOCUMENTATION PAGE</b>			<i>Form Approved OMB No. 0704-0188</i>	
Public reporting burden for this collection of information is estimated to average 1 hour per response, including the time for reviewing instruction, searching existing data sources, gathering and maintaining the data needed, and completing and reviewing the collection of information. Send comments regarding this burden estimate or any other aspect of this collection of information, including suggestions for reducing this burden, to Washington headquarters Services, Directorate for Information Operations and Reports, 1215 Jefferson Davis Highway, Suite 1204, Arlington, VA 22202-4302, and to the Office of Management and Budget, Paperwork Reduction Project (0704-0188) Washington DC 20503.				
<b>1. AGENCY USE ONLY (Leave blank)</b>		<b>2. REPORT DATE</b> March 2008	<b>3. REPORT TYPE AND DATES COVERED</b> Master's Thesis	
<b>4. TITLE AND SUBTITLE</b> Performance Analysis of an Alternative Link-16/JTIDS Waveform Transmitted Over a Channel with Pulse-Noise Interference			<b>5. FUNDING NUMBERS</b>	
<b>6. AUTHOR(S)</b> Cham Kok Kiang			<b>8. PERFORMING ORGANIZATION REPORT NUMBER</b>	
<b>7. PERFORMING ORGANIZATION NAME(S) AND ADDRESS(ES)</b> Naval Postgraduate School Monterey, CA 93943-5000				
<b>9. SPONSORING /MONITORING AGENCY NAME(S) AND ADDRESS(ES)</b> N/A			<b>10. SPONSORING/MONITORING AGENCY REPORT NUMBER</b>	
<b>11. SUPPLEMENTARY NOTES</b> The views expressed in this thesis are those of the author and do not reflect the official policy or position of the Department of Defense or the U.S. Government.				
<b>12a. DISTRIBUTION / AVAILABILITY STATEMENT</b> Approved for public release; distribution unlimited			<b>12b. DISTRIBUTION CODE</b>	
<b>13. ABSTRACT (maximum 200 words)</b> <p>The Joint Tactical Information Distribution System (JTIDS) is a hybrid frequency-hopped, direct sequence spread spectrum system that utilizes a (31,15) Reed-Solomon (RS) code and cyclical code-shift keying modulation for the data packets, where each encoded symbol consists of five bits. The primary drawback to JTIDS is the limited data rate. In this thesis, an alternative waveform consistent with the existing JTIDS channel waveform but with a two-fold increase in data rate is analyzed. The system to be considered uses (31,15) RS encoding as in the original JTIDS, but each pair of five-bit symbols at the output of the Reed-Solomon encoder undergo serial-to-parallel conversion to two five-bit symbols, which are then independently transmitted on the in-phase and quadrature components of the carrier using 32-ary biorthogonal keying with a diversity of two. The performance obtained with the alternative waveform is compared with that obtained for the existing JTIDS waveform for the relatively benign case where additive white Gaussian noise is the only noise present as well as when pulse-noise interference (PNI) is present. Errors-and-erasures decoding as well as errors-only decoding is considered. Based on the analyses, we see that the proposed alternative JITDS/Link-16 waveform performs better in AWGN as well as when PNI is present. No significant advantage is obtained using EED for the alternative waveform. There is a significant improvement in performance when perfect-side information is assumed.</p>				
<b>14. SUBJECT TERMS</b> JTIDS/Link-16, <i>M</i> -ary Bi-Orthogonal Keying, Reed-Solomon coding, Pulse-Noise Interference, Additive White Gaussian Noise, Error-and-Erasure decoding			<b>15. NUMBER OF PAGES</b> 85	
			<b>16. PRICE CODE</b>	
<b>17. SECURITY CLASSIFICATION OF REPORT</b> Unclassified	<b>18. SECURITY CLASSIFICATION OF THIS PAGE</b> Unclassified	<b>19. SECURITY CLASSIFICATION OF ABSTRACT</b> Unclassified	<b>20. LIMITATION OF ABSTRACT</b> UU	

THIS PAGE INTENTIONALLY LEFT BLANK

**Approved for public release; distribution is unlimited**

**PERFORMANCE ANALYSIS OF AN ALTERNATIVE LINK-16/JTIDS  
WAVEFORM TRANSMITTED OVER A CHANNEL WITH PULSE-NOISE  
INTERFERENCE**

Kok Kiang Cham  
Civilian, Defence Science & Technology Agency (DSTA), Singapore  
B.Eng. (EE), Nanyang Technological University, Singapore, 2001

Submitted in partial fulfillment of the  
requirements for the degree of

**MASTER OF SCIENCE IN ELECTRICAL ENGINEERING**

from the

**NAVAL POSTGRADUATE SCHOOL  
March 2008**

Author: Kok Kiang Cham

Approved by: R. Clark Robertson  
Thesis Advisor

Roberto Cristi  
Second Reader

Jeffrey B. Knorr  
Chairman, Department of Electrical and Computer Engineering

THIS PAGE INTENTIONALLY LEFT BLANK

## ABSTRACT

The Joint Tactical Information Distribution System (JTIDS) is a hybrid frequency-hopped, direct sequence spectrum system that utilizes a (31,15) Reed-Solomon (RS) code and cyclical code-shift keying modulation for the data packets, where each encoded symbol consists of five bits. The primary drawback to JTIDS is the limited data rate. In this thesis, an alternative waveform consistent with the existing JTIDS channel waveform but with a two-fold increase in data rate is analyzed. The system to be considered uses (31,15) RS encoding as in the original JTIDS, but each pair of five-bit symbols at the output of the Reed-Solomon encoder undergo serial-to-parallel conversion to two five-bit symbols, which are then independently transmitted on the in-phase and quadrature components of the carrier using 32-ary biorthogonal keying with a diversity of two. The performance obtained with the alternative waveform is compared with that obtained for the existing JTIDS waveform for the relatively benign case where additive white Gaussian noise is the only noise present as well as when pulse-noise interference (PNI) is present. Errors-and-erasures decoding as well as errors-only decoding is considered.

Based on the analyses, we see that the proposed alternative JTIDS/Link-16 waveform performs better in AWGN as well as when PNI is present. No significant advantage is obtained using EED for the alternative waveform. There is a significant improvement in performance when perfect-side information is assumed.

THIS PAGE INTENTIONALLY LEFT BLANK



## TABLE OF CONTENTS

<b>I.</b>	<b>INTRODUCTION.....</b>	<b>1</b>
A.	OVERVIEW .....	1
B.	THESIS OBJECTIVE .....	1
C.	THESIS OUTLINE.....	2
<b>II.</b>	<b>BACKGROUND .....</b>	<b>5</b>
A.	M-ARY BIORTHOGONAL SIGNALS .....	5
B.	PERFORMANCE OF M-BOK IN AWGN .....	7
C.	PERFORMANCE IN AWGN WITH PULSED-NOISE INTERFERENCE.....	7
D.	PERFORMANCE WITH DIVERSITY .....	8
E.	FORWARD ERROR CORRECTION CODING .....	9
F.	ERRORS-AND-ERASURES DECODING .....	11
G.	PERFECT-SIDE INFORMATION .....	13
H.	CHAPTER SUMMARY.....	13
<b>III.</b>	<b>PERFORMANCE OF ALTERNATIVE JTIDS/LINK-16 WAVEFORM IN SINGLE-PULSE STRUCTURE                   15</b>	
A.	PERFORMANCE OF 32-BOK WITH (31,15) RS CODING IN AWGN.....	15
B.	PERFORMANCE IN AWGN AND PULSE-NOISE INTERFERENCE.....	16
C.	PERFORMANCE WITH ERRORS-AND-ERASURES DECODING IN AWGN .....	21
D.	PERFORMANCE WITH ERRORS-AND-ERASURES DECODING IN AWGN AND PULSE-NOISE INTERFERENCE .....	26
E.	CHAPTER SUMMARY.....	32
<b>IV.</b>	<b>PERFORMANCE OF THE ALTERNATIVE JTIDS/LINK-16 WAVEFORM WITH DIVERSITY TWO (DOUBLE-PULSE STRUCTURE) ..</b>	<b>33</b>
A.	PERFORMANCE IN AWGN WITH A DIVERSITY OF TWO.....	33
B.	PERFORMANCE IN AWGN AND PNI WITH A DIVERSITY OF TWO.....	35
C.	PERFORMANCE IN AWGN AND PNI WITH A DIVERSITY OF TWO AND EED.....	39
D.	PERFORMANCE WITH PERFECT-SIDE INFORMATION IN AWGN AND PNI.....	49
E.	CHAPTER SUMMARY.....	51
<b>V.</b>	<b>COMPARISON OF THE JTIDS/LINK-16 WAVEFORM AND THE ALTERNATIVE JTIDS/LINK-16 WAVEFORM .....</b>	<b>53</b>
A.	COMPARISON OF JTIDS/LINK-16 AND THE ALTERNATIVE JTIDS/LINK-16 WAVEFROM, SINGLE-PULSE STRUCTURE.....	53
1.	Comparison for AWGN .....	53

2.	Comparison in AWGN and PNI.....	54
3.	Performance using EED in AWGN and PNI .....	56
B.	COMPARSION OF THE JTIDS/LINK-16 AND THE ALTERNATIVE JTIDS/LINK-16 WAVEFROM, DOUBLE-PULSE STRUCTURE.....	58
1.	Comparison in AWGN .....	58
2.	Performance Comparison in AWGN and PNI.....	59
3.	Performance with EED in AWGN and PNI.....	61
4.	Performance with PSI in AWGN and PNI.....	63
C.	CHAPTER SUMMARY.....	64
VI.	CONCLUSIONS AND FUTURE RESEARCH AREAS .....	65
A.	CONCLUSIONS .....	65
B.	FUTURE RESEARCH AREAS .....	66
	LIST OF REFERENCES .....	67
	INITIAL DISTRIBUTION LIST .....	69

## LIST OF FIGURES

Figure 1.	Block diagram of a $M$ -ary biorthogonal receiver.....	6
Figure 2.	Performance of the coded and uncoded alternative JTIDS/Link-16 waveform. ....	16
Figure 3.	Performance of the coded and uncoded alternative JTIDS/Link-16 waveform for $\rho = 1$ and $E_b / N_0 = 9$ dB. ....	18
Figure 4.	Performance of the coded and uncoded alternative JTIDS/Link-16 waveform for $\rho = 0.2$ and $E_b / N_0 = 9$ (dB) . ....	19
Figure 5.	Performance of 32-BOK with (31,15) RS coding in PNI with $E_b / N_0 = 6$ dB for different values of $\rho$ . ....	20
Figure 6.	Performance of 32-BOK with (31,15) RS coding in PNI with $E_b / N_0 = 9$ dB for different values of $\rho$ . ....	21
Figure 7.	Performance of 32-BOK with (31,15) RS coding and EED for different values of $a$ in the presence of AWGN.....	26
Figure 8.	Performance of 32-BOK with (31,15) RS coding and EED for $\rho = 1$ and $E_b / N_0 = 6$ dB for different values of $a$ . ....	29
Figure 9.	Performance of 32-BOK with (31,15) RS coding with EED in a PNI environment for $a = 0.6$ and $E_b / N_0 = 6$ dB.....	30
Figure 10.	Performance of 32-BOK with RS coding with and without EED with $E_b / N_0 = 6$ dB and $a = 0.6$ for different $\rho$ .....	31
Figure 11.	Performance of 32-BOK with (31,15) RS coding with and without EED with $E_b / N_0 = 6$ dB and $a = 0.4$ for different values of $\rho$ . ....	32
Figure 12.	Performance of 32-BOK with (31,15) RS coding for both the single-pulse and the double-pulse structure in AWGN.....	34
Figure 13.	Performance of 32-BOK with (31,15) RS coding and the double-pulse structure for different $\rho$ with $E_c / N_0 = 2.4$ dB.....	37
Figure 14.	Performance of 32-BOK with (31,15) RS coding and the double-pulse structure for different $\rho$ with $E_c / N_0 = 3$ dB .....	38
Figure 15.	Performance of 32-BOK with (31,15) RS coding for both the double-pulse structure ( $E_c / N_0 = 2.4$ dB) and the single-pulse structure ( $E_b / N_0 = 5.4$ dB).....	39
Figure 16.	Performance of 32-BOK with (31,15) RS coding and EED for the double-pulse structure with $\rho = 0.5$ and $E_c / N_0 = 2.5$ dB for different values of $a$ ...	43
Figure 17.	Performance of 32-BOK with (31,15) RS coding and EED for the double-pulse structure with $\rho = 0.5$ and $E_c / N_0 = 15$ dB for different values of $a$ ....	44
Figure 18.	Performance of 32-BOK with (31,15) RS coding and EED ( $E_b / N_0 = 2.5$ dB, $a = 0.6$ ) for the double-pulse structure.....	45

Figure 19.	Performance of 32-BOK with (31,15) RS coding and EED ( $E_b / N_0 = 15$ dB, $a = 0.6$ ) for the double-pulse structure.....	46
Figure 20.	Performance of 32-BOK with (31,15) RS coding, EED, $a = 0.6$ , for $\rho = 1$ for the double-pulse ( $E_c / N_0 = 2.5$ dB) and the single-pulse structure ( $E_c / N_0 = 5.5$ dB).....	47
Figure 21.	Performance of 32-BOK with (31,15) RS coding with and without EED with $E_c / N_0 = 2.5$ dB and $a = 0.6$ for different values of $\rho$ .....	48
Figure 22.	Performance of 32-BOK with (31,15) RS coding with and without EED with $E_c / N_0 = 15$ dB and $a = 0.6$ for different values of $\rho$ .....	49
Figure 23.	Performance for 32-BOK with (31,15) RS coding with and without PSI for different $\rho$ ( $E_c / N_0 = 2.5$ dB).....	51
Figure 24.	Performance of 32-BOK with (31,15) RS coding and JTIDS/Link-16 in AWGN.....	54
Figure 25.	Performance of 32-BOK with (31,15) RS coding ( $E_b / N_0 = 5.5$ dB) and JTIDS waveform ( $E_b / N_0 = 7.6$ dB) for different values of $\rho$ .....	55
Figure 26.	Performance of the alternative JTIDS/LINK-16 waveform ( $a = 0.6$ , $E_b / N_0 = 5.5$ dB) and the JTIDS/Link-16 waveform with EED (threshold=14, $E_b / N_0 = 7.3$ dB) for different values of $\rho$ .....	56
Figure 27.	Performance of the alternative JTIDS/Link-16 waveform ( $a = 0.6$ ) and the JTIDS/Link-16 waveform (threshold=14) with EED at $E_b / N_0 = 7.3$ dB for $\rho = 1$ and 0.5.....	57
Figure 28.	Performance of the alternative JTIDS/Link-16 waveform and the JTIDS waveform for the double-pulse structure.....	59
Figure 29.	Performance of the alternative JTIDS/Link-16 waveform ( $E_c / N_0 = 2.4$ dB) and the JTIDS/Link-16 waveform ( $E_c / N_0 = 4.5$ dB) for the double-pulse structure.....	60
Figure 30.	Performance of the alternative JTIDS/LINK-16 waveform ( $a = 0.6$ , $E_c / N_0 = 2.5$ dB) and the JTIDS/Link-16 waveform (threshold=14, $E_c / N_0 = 4.4$ dB) with EED.....	61
Figure 31.	Performance of the alternative JTIDS/Link-16 waveform ( $a = 0.6$ ) and the JTIDS/Link-16 waveform (threshold=14) with EED at $E_c / N_0 = 4.4$ dB.....	63
Figure 32.	Performance for the alternative JTIDS/Link-16 (PSI, $E_c / N_0 = 2.5$ dB) and the JTIDS/Link-16 waveform (EED, threshold=14, $E_c / N_0 = 4.3$ dB).....	64

## EXECUTIVE SUMMARY

Digital datalinks are the technology at the heart of modern wireless networks and are also the technological basis of systems supporting Network Centric Warfare and Network Enabled Operations. The ability to provide real time tactical data updates to all members of a network is crucial to achieving information supremacy and situational awareness in today's complex war theater.

The Joint Tactical Information Distribution System (JTIDS)/Link-16 is an advanced tactical datalink that is used by a number of different countries. It provides both voice and data communications for command and control, navigation, relative positioning, and identification. JTIDS/Link-16 is a time-division, multiple access communication system operating at L-band frequencies.

Many techniques are used in JTIDS. These include the use of Reed Solomon encoding for error detection and correction, frequency hopping and direct sequence spread spectrum techniques that makes JTIDS more resistant to jamming, and data encryption to make it a secure data network. Only a small fraction of the available radio bandwidth in the L band is used at any one time as a result of frequency hopping. In direct-sequence spread spectrum, each digital symbol is represented by a pseudo-random sequence for transmission. This reduces the amount of achievable data throughput per radio bandwidth in proportion to the length of the pseudo-random spreading code. Thus, while both frequency hopping and direct sequence spread spectrum provide JTIDS with jam-resistance, the effective data throughput is reduced. As a digital system for both data and voice, JTIDS needs to handle large amounts of data - far more than the communication systems now used for similar purposes.

Throughput is one of the basic measures of performance for any datalink or digital communications system and is linked to the type of modulation used. JTIDS uses *cyclic code-shift keying* (CCSK) and *minimum-shift keying* (MSK), which is a type of continuous *phase-shift modulation* (CPSM), to modulate the digital data. The data are first encoded using a (31,15) Reed Solomon code. These coded symbols are interleaved

and modulated using a set of CCSSK code symbols to produce 32-chip sequences. The chips are transmitted using MSK. The primary drawback to JTIDS is a large overhead which results in a limited data rate.

In this thesis, an alternative waveform that is consistent with the existing JTIDS channel waveform but with a two-fold increase in data rate is analyzed. The system to be considered uses (31,15) Reed Solomon encoding as in the original JTIDS, but each pair of the five-bit symbols at the output of the Reed Solomon encoder undergo a serial-to-parallel conversion to two five-bit symbols. They are then independently transmitted on the in-phase and quadrature components of the carrier using 32-ary bi-orthogonal keying (32-BOK) with a diversity of two. As a result, this system supports a data rate of twice that of the existing JTIDS waveform and is consistent with the direct sequence waveform generated by JTIDS. The performance obtained with alternative waveform is compared with that obtained with the existing JTIDS waveform for the relatively benign case where AWGN is the only noise present as well as when pulse-noise interference (PNI) is present. Errors and erasure decoding as well as errors-only decoding is considered.

Based on the results of this thesis, the proposed alternative JTIDS/Link-16 waveform has better performance than the existing JTIDS/Link-16 waveform in AWGN as well as when pulse-noise interference (PNI) is present. There is no significant advantage in using EED for the alternative waveform either in only AWGN or with both AWGN and PNI. There is a significant improvement in performance when PNI is present and perfect-side information is assumed.

## **ACKNOWLEDGMENTS**

I would like to express my utmost gratitude to Professor Clark Robertson of the Naval Postgraduate School, Monterey, California, for his guidance, patience and contribution to the successful completion of this thesis work.

I would also like to thank Professor Roberto Cristi for serving as my second reader and reviewing this thesis.

I would also like to thank my parents for their support and encouragement.

Last, but not least, I must thank my sponsor, Defence Science and Technology Agency (DSTA), for providing me the opportunity to pursue my work here in the Naval Postgraduate School.

THIS PAGE INTENTIONALLY LEFT BLANK



# **I. INTRODUCTION**

## **A. OVERVIEW**

Digital datalinks are the technology at the heart of modern wireless networks and are also the technological basis of systems supporting Network Centric Warfare and Network Enabled Operations. The ability to provide real time tactical data updates to all members of a network is crucial to achieving information supremacy and situational awareness in today's complex war theater.

The Joint Tactical Information Distribution System (JTIDS)/Link-16 is one of the most advanced tactical datalinks that is in use in today's armed forces. It provides both voice and data communications for command and control, navigation, relative positioning, and identification. JTIDS/Link-16 is a time-division, multiple access communication system operating at L-band frequencies [1].

JTIDS/Link-16 uses (31,15) Reed-Solomon (RS) encoding and cyclic code shift keying (CCSK) modulation for data packets, where each encoded symbol consists of five bits and is spread into 32 chips per symbol for transmission using minimum-shift keying (MSK) modulation. The primary drawback to JTIDS/Link-16 is the limited data rate that can be achieved.

## **B. THESIS OBJECTIVE**

Numerous studies of ways to increase the data rate of the JTIDS/Link-16 throughput have been made. One example is Link-16 Enhanced Throughput (LET), which works by replacing the spread spectrum and RS encoding of the original JTIDS waveform with a RS/convolutional coding scheme which can adapt to required link capability [2] [3]. However, this increase in data rate is at the expense of both jamming resistance and transmission range. Thus, LET may not prove practical for combat scenarios. Other papers [4], [5], [6] related to JTIDS include comparison of a CCSK waveform with an orthogonal waveform [4] and an analysis of different error-control

coding techniques for high-rate direct sequence spread spectrum [5]. In [6], the authors derive an analytical approximation for the probability of symbol error for a CCSK waveform with RS coding. In [7], this approximation is shown to be optimistic by about 2 dB. To the best of the author's knowledge, the analysis of a JTIDS/Link-16 compatible waveform obtained by replacing CCSK with  $M$ -ary bi-orthogonal keying ( $MBOK$ ) and taking into account pulse-noise interference has not been previously investigated. The objective of this thesis is to investigate an alternative physical layer channel waveform that is compatible with the existing JTIDS channel waveform but with the potential to increase the data rate by a factor of two as well as reduce the required signal-to-noise ratio.

The alternative JTIDS/Link-16 waveform investigated utilizes a complex  $MBOK$  waveform with  $(n, k)$  RS coding.  $MBOK$  can be thought of as a hybrid of  $M$ -ary orthogonal modulation and binary phase-shift keying (BPSK). The data first undergoes forward error coding (FEC) using RS coding, and the coded data undergoes serial-to-parallel conversion to two five-bit symbols which are independently modulated with  $MBOK$  on the in-phase (I) and quadrature (Q) components of the carrier. To be consistent with JTIDS/Link-16 waveform, we use 32-BOK and a (31,15) RS code. The proposed waveform provides a two-fold increase in the data rate with the same spectral efficiency as the JTIDS/Link-16 waveform. The performance of the proposed alternative JTIDS/Link-16 waveform is compared to the results of the existing JTIDS/Link-16 waveform in [7] both when AWGN is the only noise present as well as with PNI. The performance of the alternative waveform for both single as well as dual diversity is examined.

## C. THESIS OUTLINE

The introduction to the thesis was presented in this chapter. The alternative waveform is discussed in Chapter II. The performance analysis of the alternative waveform with RS coding and no diversity is presented in Chapter III. The performance analysis of the alternative waveform with RS coding and a diversity of two is discussed

in Chapter IV, and the performance of the alternative JTIDS/Link-16 waveform and that of the JTIDS/Link-16 waveform with no diversity as well as with a diversity of two, for both an AWGN and a PNI environment, are compared in Chapter V. The thesis conclusions based on the results obtained are presented in Chapter VI.

THIS PAGE INTENTIONALLY LEFT BLANK

## II. BACKGROUND

In this chapter, we introduce some of the background knowledge and concepts required for our subsequent analysis of the alternative JTIDS/Link-16 waveform considered in this thesis.

### A. M-ARY BIORTHOGONAL SIGNALS

A set of  $M$  biorthogonal signals can be constructed from  $M/2$  orthogonal signals by including the negatives of each of the orthogonal signals. Thus, a biorthogonal set is really two sets of orthogonal codes such that each symbol in one set has its antipodal symbol in the other set. One advantage of biorthogonal modulation over orthogonal modulation for the same data is that biorthogonal modulation requires one-half as many chips per symbol. Thus, the bandwidth requirement for biorthogonal modulation is one-half of that required for comparable orthogonal modulation. Since antipodal signal vectors have better distance properties than orthogonal ones, biorthogonal modulation performs slightly better than orthogonal modulation [8].

The channel waveform for complex MBOK can be represented by

$$s(t) = \pm A_c c_i(t) \cos(2\pi f_c t + \theta) - (\pm) A_c c_j(t) \sin(2\pi f_c t + \theta) \quad (2.1)$$

which is transmitted for  $T_s = 2kT_b$  seconds,  $2k$  is the number of bits in each symbol, and  $c_x(t)$  represents a waveform of  $2^{k-1}$  pulses of duration  $T_c = T_s / 2^{k-1}$ , where  $i$  or  $j$  may or may not be different depending on the data bits. Clearly, complex  $2^k$ -BOK is equivalent to transmitting  $2^k$ -BOK independently on both the I and Q components of the carrier, so complex  $2^k$ -BOK is actually a  $2^{2k}$ -ary modulation technique.

A block diagram of a  $M$ -ary biorthogonal receiver is shown in Figure 1.

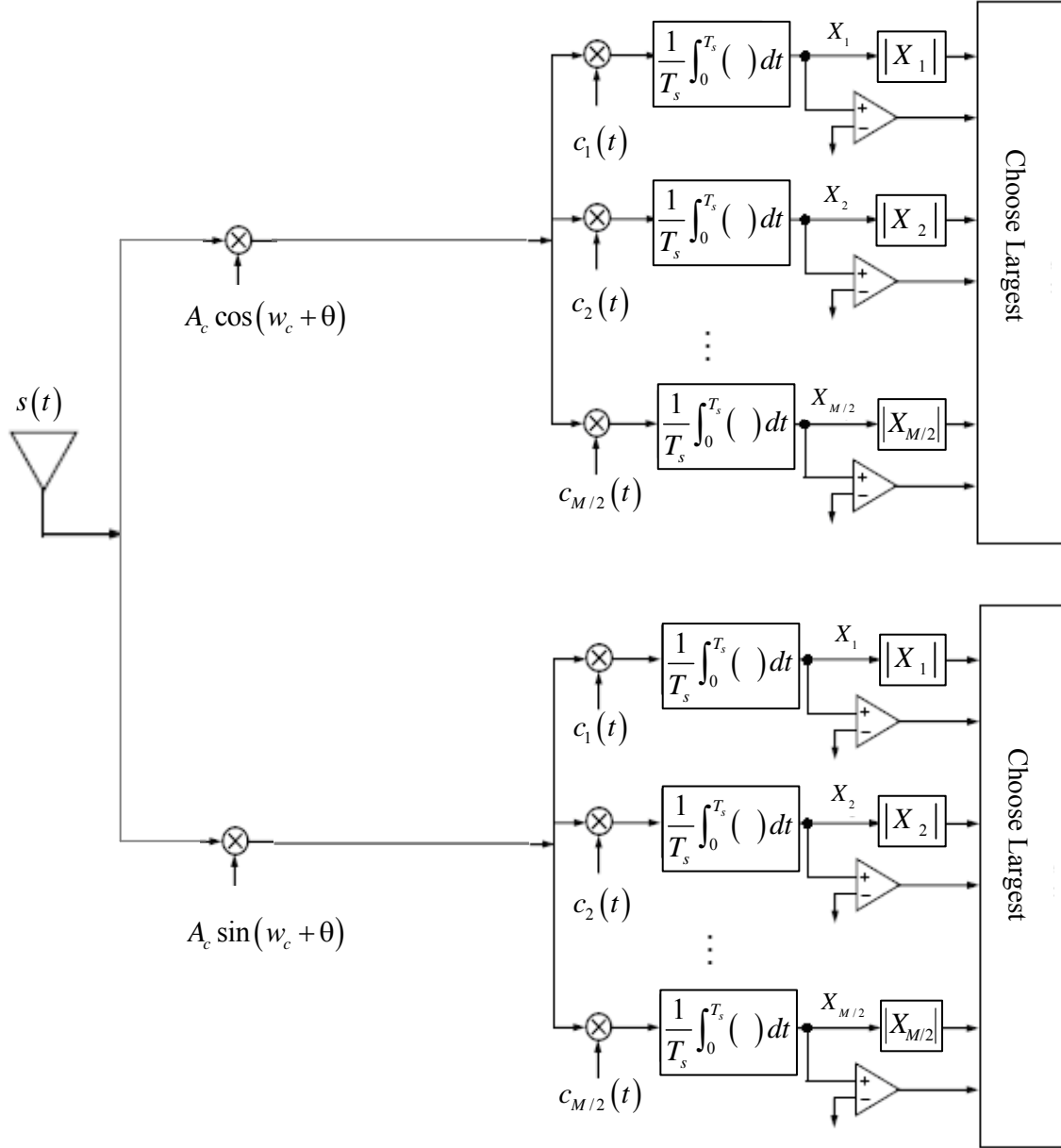


Figure 1. Block diagram of a  $M$ -ary biorthogonal receiver.

The conditional probability density function for the random variables  $X_m$  where  $m = 1, 2, \dots, M/2$ , that represents the integrator outputs when the noise can be considered Gaussian noise are

$$f_{x_m}(x_m | m) = \frac{1}{\sqrt{2\pi\sigma}} \exp \left[ \frac{-(x_m - \sqrt{2}A_c)^2}{2\sigma^2} \right] \quad \text{for } m \leq M/2, \quad (2.2)$$

$$f_{x_m}(x_m | m) = \frac{1}{\sqrt{2\pi\sigma}} \exp \left[ \frac{-(x_m + \sqrt{2}A_c)^2}{2\sigma^2} \right] \quad \text{for } M/2 + 1 \leq m \leq M, \quad (2.3)$$

and

$$f_{x_n}(x_n | n, n \neq m) = \frac{1}{\sqrt{2\pi\sigma}} \exp \left[ \frac{-x_n^2}{2\sigma^2} \right] \quad (2.4)$$

where  $\sigma^2 = N_0 / T_s$ .

## B. PERFORMANCE OF M-BOK IN AWGN

When AWGN is present with power spectral density  $N_0/2$ , the probability of channel symbol error for MBOK in AWGN is [9]

$$p_s = 1 - \frac{1}{\sqrt{2\pi}} \int_{-\sqrt{2E_s/N_0}}^{\infty} e^{-\frac{u^2}{2}} \left[ 1 - 2Q(u + \sqrt{\frac{2E_s}{N_0}}) \right]^{\frac{M}{2}-1} du \quad (2.5)$$

where  $E_s$  is the average energy per channel symbol, which is equal to  $A_c^2 T_s$ , where  $A_c^2$  is the average received signal power,  $T_s$  is the symbol duration, and  $Q(\bullet)$  is the Q-function. Equation (2.5) will be used for deriving the probability of symbol and bit error for the alternative JTIDS/Link-16 system in the next chapter.

## C. PERFORMANCE IN AWGN WITH PULSED-NOISE INTERFERENCE

For military applications, it is imperative that we also consider the performance of the system when subjected to PNI. In this thesis, we consider the performance of the alternative JTIDS/Link-16 system in AWGN as well as PNI.

When a channel is affected by AWGN, the noise signal that arrives at the receiver is assumed to be uniformly spread across the spectrum and time-independent. When there

is PNI in the channel, the preceding assumptions may not be valid. The total noise power at the receiver integrator outputs when both AWGN and PNI are present is given by

$$\sigma_x^2 = \sigma_o^2 + \sigma_I^2 \quad (2.6)$$

where  $\sigma_o^2 = N_0 / T_b$  and  $\sigma_I^2 = N_I / \rho T_b$ , and  $\rho$  is the fraction of time that a narrowband Gaussian noise interferer is switched on. In the event  $\rho=1$  the PNI is barrage noise interference since it is on continuously.

Consequently, the probability of symbol error when a signal experiences PNI can be expressed as

$$P_s = \Pr(\text{Interferer is OFF}) p_s(\text{AWGN}) + \Pr(\text{Interferer is ON}) p_s(\text{AWGN+PNI}) \quad (2.7)$$

$$P_s = (1-\rho) p_s(\text{AWGN}) + \rho p_s(\text{AWGN+PNI}) \quad (2.8)$$

where  $p_s(x)$  represent the probability of symbol error for condition  $x$ . The equations assume that a symbol is either completely free of interference or is interfered with for an entire symbol.

#### D. PERFORMANCE WITH DIVERSITY

JTIDS/Link-16 employs several techniques to increase immunity to an adversary's interference. One of the techniques used is diversity. While there are many ways in which diversity can be implemented, in JTIDS/Link-16, this is implemented as a simple repetition code, referred to as either the single pulse (no diversity) or the standard double pulse (STDP) structure (sequential diversity of two). For the STDP, the transmitter transmits the same symbol twice at different carrier frequencies, thus providing redundancy at the receiver. In order for diversity to be effective, each redundant symbol must be received independently [10]. There are four basic JTIDS message formats used, of which the STDP message provides the best jam-resistance capability. STDP are transmitted twice at different carrier frequencies not only to achieve



redundancy for improved interference resistance but also to compensate for propagation problems or antenna coverage limitations in maneuvering platforms [2].

When diversity of order  $L$  is employed and each diversity signal is received independently, the probability that  $i$  of  $L$  diversity receptions are affected by PNI, where  $\rho$  represents the fraction of time the channel is affected by PNI, is represented as [11]

$$\Pr(i \text{ of } L \text{ pulses jammed}) = \binom{L}{i} \rho^i (1-\rho)^{L-i} \quad (2.9)$$

where there are  $\binom{L}{i}$  different ways in which  $i$  of  $L$  diversity receptions can be received in error.

Consequently, the probability of symbol error for a system with diversity  $L$  in the presence of PNI is

$$P_s = \sum_{i=0}^L [\Pr(i \text{ of } L \text{ signals jammed}) p_s(i)] \quad (2.10)$$

which is given explicitly by

$$P_s = \sum_{i=0}^L \left[ \binom{L}{i} \rho^i (1-\rho)^{L-i} p_s(i) \right] \quad (2.11)$$

where  $p_s(i)$  is the conditional probability of symbol error given  $i$  of  $L$  diversity receptions are affected by the PNI.

## **E. FORWARD ERROR CORRECTION CODING**

In a binary system that utilizes block FEC coding,  $n$  coded bits are transmitted in the time it otherwise takes to transmit  $k$  information bits. At the receiver, the decoder is able to correct up to  $t$  bits errors in every block of  $n$  coded bits.

For JTIDS/Link-16, the FEC used is (31,15) RS coding, a linear, non-binary code. To maintain consistency with the JTIDS/Link-16 waveform, the alternative JTIDS/Link-16 waveform also employs (31,15) RS coding for error detection and correction. RS

codes are non-binary Bose-Chaudhuri-Hocquenghem (BCH) codes. For non-binary codes,  $m$  bits at a time are combined to form a symbol, an  $(n, k)$  RS encoder takes  $k$  information symbols ( $mk$  information bits) and generates  $n$  coded symbols ( $mn$  coded bits).

For  $(n, k)$  RS coding, the probability of decoder error, or block error, is upper bounded by the sum of the probabilities that a received code word differs from the correct code word by  $i$  symbols for all  $i > t$  [12]. Therefore,

$$P_E \leq \sum_{j=t+1}^n \binom{n}{j} p_s^j (1-p_s)^{n-j} \quad (2.12)$$

or

$$P_E \leq 1 - \sum_{j=0}^t \binom{n}{j} p_s^j (1-p_s)^{n-j} \quad (2.13)$$

where the inequality holds for either a perfect code or a bounded distance decoder,  $t$  is the symbol-error correcting capability of the code, and  $p_s$  is the channel symbol error probability.

Assuming that the probability of information symbol error given  $j$  code symbol errors is approximately  $j/n$ , we obtain the probability of information symbol error as

$$P_s \approx \frac{1}{n} \sum_{j=t+1}^n j \binom{n}{j} p_s^j (1-p_s)^{n-j} \quad (2.14)$$

For as  $(n, k)$  RS code, we can also express (2.14) as

$$P_s \approx \frac{1}{2^m - 1} \sum_{j=t+1}^{2^m-1} j \binom{2^m-1}{j} p_s^j (1-p_s)^{2^m-1-j} \quad (2.15)$$

where  $m$  represents the number of bits per symbol.

We can approximate the probability of bit error by taking the average of the upper and lower bound on the probability of bit error given that a symbol error has occurred to obtain

$$P_b \approx \frac{m+1}{2m} P_s \quad (2.16)$$

Either equation (2.14) or (2.15) can be used with (2.16) to obtain the probability of symbol error for the alternative JTIDS/Link-16 waveform.

## F. ERRORS-AND-ERASURES DECODING

Error-and-erasures (EED) is one of the simplest forms of soft decision decoding. The implementation of EED is such that, for symbols that are received ambiguously, an erasure is declared. Thus, the number of possible outputs is the number of symbols plus an erasure. For example, in binary erasure decoding, the output of the demodulator is not binary but ternary. The three possible outputs are bit 1, 0 and erasure ( $e$ ). Suppose that a received code word has a single erased bit. Now all valid code words are separated by a Hamming distance of at least  $d_{\min} - 1$ , where  $d_{\min}$  is the minimum Hamming distance of the code. In general, given  $i$  erasures in a received code word, all valid code words are separated by a Hamming distance of at least  $d_{\min} - i$ . Hence, the effective free distance between valid code words is

$$d_{\min, \text{eff}} = d_{\min} - i \quad (2.17)$$

Therefore, the number of errors  $j$  in the non-erased bits of the code word that can be corrected is given by

$$t_c = \frac{1}{2} \lfloor d_{\min} - e - 1 \rfloor \quad (2.18)$$

where  $\lfloor x \rfloor$  implies rounding  $x$  down. Thus, a combination of  $t_e$  errors and  $e$  erasures can be corrected as long as

$$2t_e + e < d_{\min} \quad (2.19)$$

Hence, twice as many erasures as errors can be corrected. Intuitively, this makes sense because we have more information about the erasures; the locations of erasures are known, but the locations of errors are not.

For error-and-erasures decoding, the probability that there are a total of  $i$  errors and  $j$  erasures in a block of  $n$  symbols is given by

$$\Pr(i, j) = \binom{n}{i} \binom{n-i}{j} p_s^i p_e^j p_c^{n-i-j} \quad (2.20)$$

where each symbol is assumed to be received independently,  $p_e$  is the probability of channel symbol erasure,  $p_s$  is the probability of channel symbol error, and  $p_c$  is the probability of correct channel symbol detection. The probability of channel error can be obtained from

$$p_s = 1 - p_e - p_c \quad (2.21)$$

Since a block error does not occur as long as  $d_{\min} > 2i + j$ , then the probability of correct block decoding is given by

$$P_C = \sum_{i=0}^t \binom{n}{i} p_s^i \sum_{j=0}^{d_{\min}-1-2i} \binom{n-i}{j} p_e^j p_c^{n-i-j} \quad (2.22)$$

This gives the probability of block error as

$$P_E = 1 - P_C \quad (2.23)$$

which is

$$P_E = 1 - \sum_{i=0}^t \binom{n}{i} p_s^i \sum_{j=0}^{d_{\min}-1-2i} \binom{n-i}{j} p_e^j p_c^{n-i-j} \quad (2.24)$$

Using (2.24), we can approximate the probability of symbol error by taking the average of the upper and lower bound on the probability of symbol error given that a block error has occurred to obtain

$$P_s \approx \frac{k+1}{2k} P_E \quad (2.25)$$

Similarly, we can approximate the probability of bit error by taking the average of the upper and lower bound on the probability of bit error given that a symbol error has occurred, previously given by (2.16).

## **G. PERFECT-SIDE INFORMATION**

For a system with a diversity of  $i$ , where the diversity receptions are received independently, perfect-side information (PSI) modulation can be considered. In the case of the double-pulse structure, when both received symbols in the repetitive pulses are not affected by PNI, they are combined and demodulated. If either of the diversity receptions suffers from PNI, the receiver discards the PNI-affected symbol and makes its decision based on a single-pulse with AWGN. When both diversity receptions are affected by PNI, the receiver recovers the signal in the normal fashion. PSI requires at least a diversity of two and can improve the performance of the system in an pulse-noise environment where  $\rho < 1$ .

## **H. CHAPTER SUMMARY**

In this chapter, we introduced biorthogonal signals and addressed the background and concepts necessary to examine the performance of an alternative JTIDS/Link-16 waveform which consists of complex 32-BOK with (31,15) RS coding. The concept of diversity, EED as well as the concept of PSI was introduced. In the next chapter, we examine the performance of an alternative JTIDS waveform that utilizes (31,15) RS coding with *MBOK* modulation transmitted over both a channel with only AWGN as well as channel with both AWGN and PNI. The single-pulse structure (no diversity) is considered in the next chapter.

THIS PAGE INTENTIONALLY LEFT BLANK

### III. PERFORMANCE OF ALTERNATIVE JTIDS/LINK-16 WAVEFORM IN SINGLE-PULSE STRUCTURE

In this chapter, we investigate the performance of an alternative JTIDS/Link-16 waveform by analyzing the probability of bit error vs.  $E_b / N$  for AWGN as well as AWGN plus PNI. The performance using EED is also to be analyzed. The analyses for this chapter consider only the case of no diversity.

#### A. PERFORMANCE OF 32-BOK WITH (31,15) RS CODING IN AWGN

The probability of symbol error for  $M$ -BOK is given in (2.5). For the alternative JTIDS system that uses (31,15) RS coding, the probability of channel symbol error for is

$$p_s = 1 - \frac{1}{\sqrt{2\pi}} \int_{-\sqrt{2rE_s/N_0}}^{\infty} e^{-\frac{u^2}{2}} \left[ 1 - 2Q\left(u + \sqrt{\frac{2rE_s}{N_0}}\right) \right]^{\frac{M}{2}-1} du \quad (3.1)$$

Expressed in terms of bit energy  $E_b$  we have

$$p_s = 1 - \frac{1}{\sqrt{2\pi}} \int_{-\sqrt{2rmE_b/N_0}}^{\infty} e^{-\frac{u^2}{2}} \left[ 1 - 2Q\left(u + \sqrt{\frac{2rmE_b}{N_0}}\right) \right]^{\frac{M}{2}-1} du \quad (3.2)$$

$$p_s = 1 - \frac{1}{\sqrt{2\pi}} \int_{-\sqrt{2rm\gamma_b}}^{\infty} e^{-\frac{u^2}{2}} \left[ 1 - 2Q\left(u + \sqrt{2rm\gamma_b}\right) \right]^{\frac{M}{2}-1} du \quad (3.3)$$

where  $m$  is the number of bits per symbol,  $r = k / n$  and  $\gamma_b = E_b / N_o$ .

Substituting (3.3) into (2.14), we obtain the probability of symbol error for MBOK with RS decoding in the presence of AWGN as

$$P_s \approx \frac{1}{n} \sum_{j=t+1}^n j \binom{n}{j} p_s^j (1 - p_s)^{n-j} \quad (3.4)$$

Using (3.4) and (2.16), we obtain an approximation for the probability of bit error.

Using (3.3), (3.4) and (2.16), we plot the results for the probability of bit error of the alternative JTIDS/Link-16 waveform in Figure 2 where  $r = 15/31$  and  $m = 5$ . For

purposes of comparison, both uncoded and coded performance is plotted. The uncoded performance is plotted using (2.5) where  $E_s = mE_b$ .

We see that at  $P_b = 10^{-5}$ , the coded waveform requires  $E_b / N_0 = 4.7$  dB, while the uncoded waveform requires  $E_b / N_0 = 6.7$  dB. Hence, there is a coding gain of 2 dB at  $P_b = 10^{-5}$ .

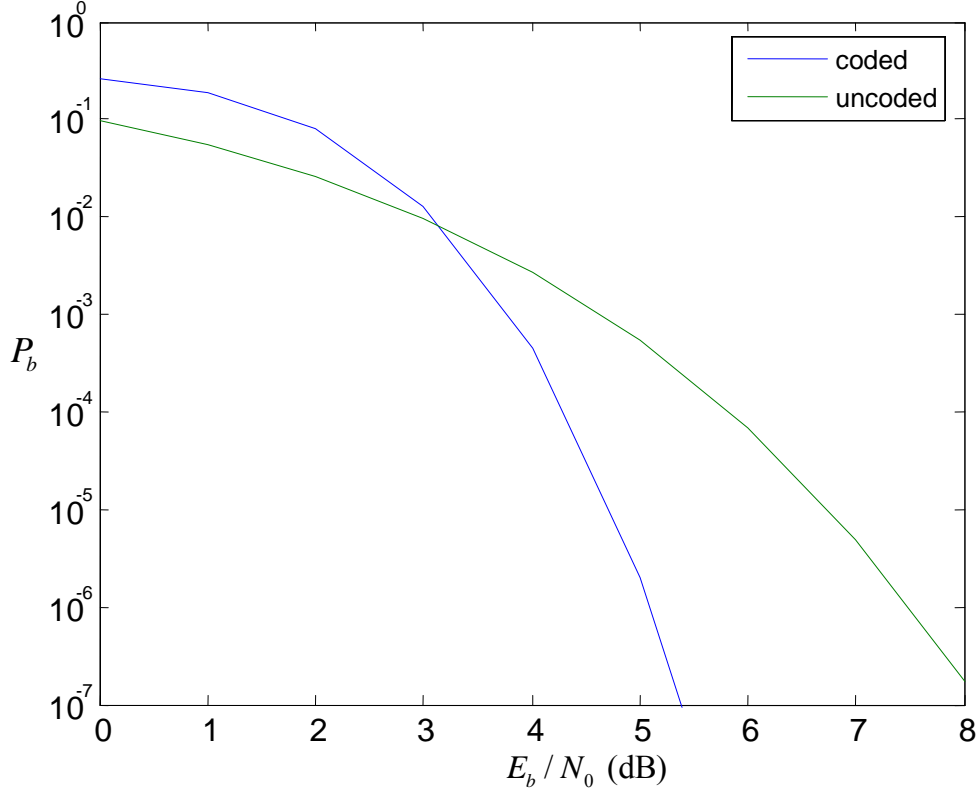


Figure 2. Performance of the coded and uncoded alternative JTIDS/Link-16 waveform.

## B. PERFORMANCE IN AWGN AND PULSE-NOISE INTERFERENCE

When the channel also has PNI, (2.6), (2.8) and (3.2) can be used to obtain the probability of channel symbol error with AWGN and PNI as either



$$\begin{aligned}
p_s = & \rho \left[ 1 - \frac{1}{\sqrt{2\pi}} \int_{-\sqrt{\frac{2rm}{\frac{N_I}{\rho E_b} + \frac{N_0}{E_b}}}}^{\infty} e^{-\frac{u^2}{2}} \left[ 1 - 2Q\left(u + \sqrt{\frac{2rm}{\frac{N_I}{\rho E_b} + \frac{N_0}{E_b}}}\right) \right]^{\frac{M}{2}-1} du \right] \\
& + (1-\rho) \left[ 1 - \frac{1}{\sqrt{2\pi}} \int_{-\sqrt{2rmE_b/N_0}}^{\infty} e^{-\frac{u^2}{2}} \left[ 1 - 2Q\left(u + \sqrt{\frac{2rmE_b}{N_0}}\right) \right]^{\frac{M}{2}-1} du \right]
\end{aligned} \tag{3.5}$$

or

$$\begin{aligned}
p_s = & \rho \left[ 1 - \frac{1}{\sqrt{2\pi}} \int_{-\sqrt{\frac{2rm}{\frac{1}{\rho\gamma_I} + \frac{1}{\gamma_b}}}}^{\infty} e^{-\frac{u^2}{2}} \left[ 1 - 2Q\left(u + \sqrt{\frac{2rm}{\frac{1}{\rho\gamma_I} + \frac{1}{\gamma_b}}}\right) \right]^{\frac{M}{2}-1} du \right] \\
& + (1-\rho) \left[ 1 - \frac{1}{\sqrt{2\pi}} \int_{-\sqrt{2rm\gamma_b}}^{\infty} e^{-\frac{u^2}{2}} \left[ 1 - 2Q\left(u + \sqrt{2rm\gamma_b}\right) \right]^{\frac{M}{2}-1} du \right]
\end{aligned} \tag{3.6}$$

where  $\gamma_I = E_b / N_I$ . Defining  $\zeta = 1/(\gamma_b^{-1} + (\rho\gamma_I)^{-1})$ , we obtain from (3.6)

$$\begin{aligned}
p_s = & \rho \left[ 1 - \frac{1}{\sqrt{2\pi}} \int_{-\sqrt{2rm\zeta}}^{\infty} e^{-\frac{u^2}{2}} \left[ 1 - 2Q\left(u + \sqrt{2rm\zeta}\right) \right]^{\frac{M}{2}-1} du \right] \\
& + (1-\rho) \left[ 1 - \frac{1}{\sqrt{2\pi}} \int_{-\sqrt{2rm\gamma_b}}^{\infty} e^{-\frac{u^2}{2}} \left[ 1 - 2Q\left(u + \sqrt{2rm\gamma_b}\right) \right]^{\frac{M}{2}-1} du \right]
\end{aligned} \tag{3.7}$$

The probability of information channel symbol error and bit error for both AWGN and PNI are obtained from (3.7), (3.4) and (2.16). Results are shown in Figure 3 for  $E_b / N_0 = 9$  dB and  $\rho = 1$ , and Figure 4 for  $E_b / N_0 = 9$  dB and  $\rho = 0.2$  for both a coded and an uncoded waveform. In Figure 3, at  $P_b = 10^{-5}$ , the required  $E_b / N_I = 6.8$  dB for the coded waveform, and for the uncoded waveform, the required  $E_b / N_I = 10.8$  dB. There is a coding gain of 4 dB. Similarly from Figure 4, for  $P_b = 10^{-5}$ , for the coded case, we

required  $E_b / N_I = 9.4$  dB, and  $E_b / N_I = 16.2$  dB for the uncoded case. There is a coding gain of 6.8 dB. From the above, we see that coding gives better performance than the uncoded waveform. Also, we observe that, while the absolute performance of the coded waveform is better when  $\rho = 1$  in comparison to that of the coded waveform when  $\rho = 0.2$ , there is a larger coding gain between the coded and uncoded waveform for  $\rho = 0.2$ .

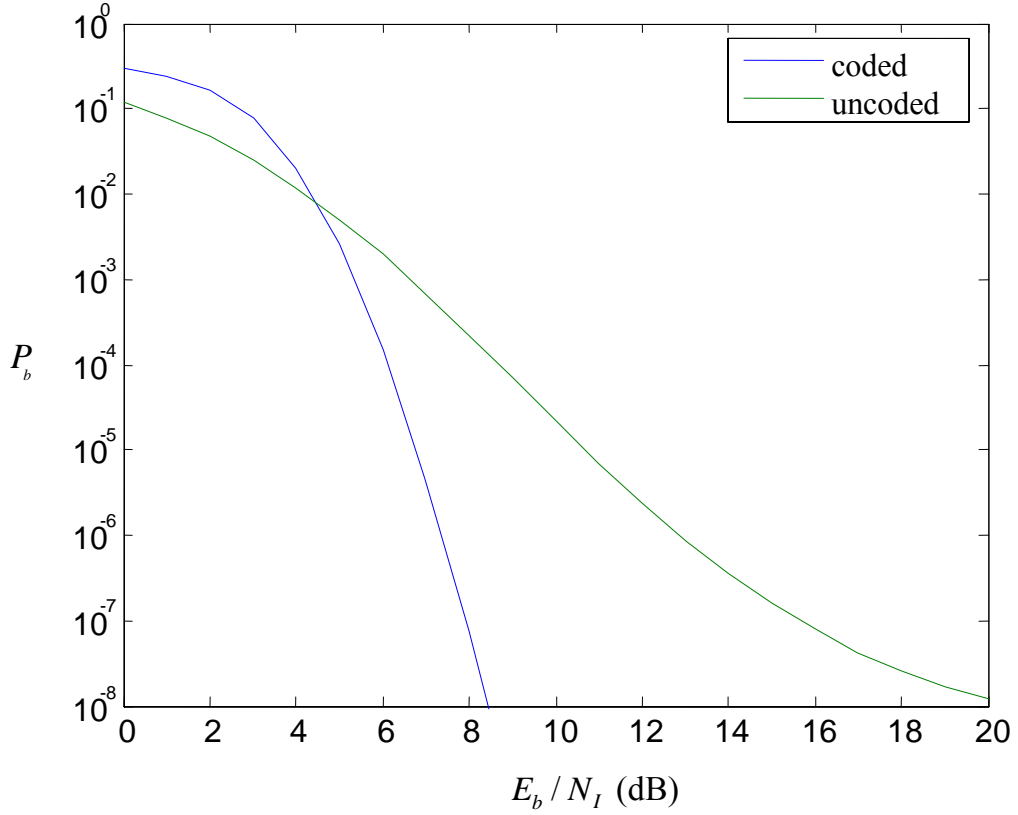


Figure 3. Performance of the coded and uncoded alternative JTIDS/Link-16 waveform for  $\rho = 1$  and  $E_b / N_0 = 9$  dB.

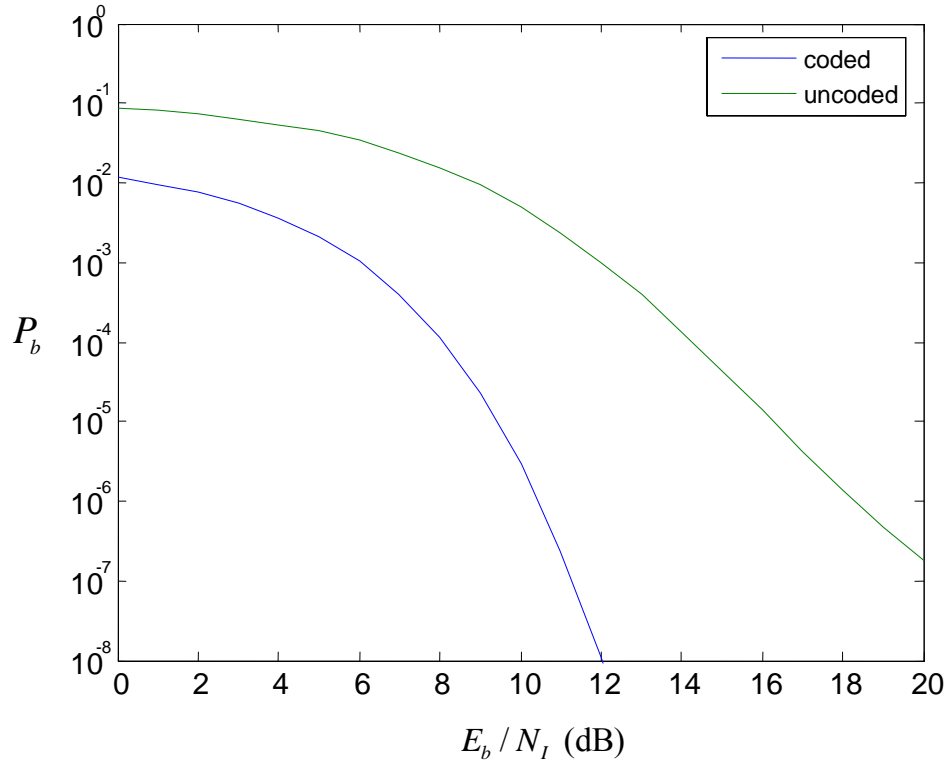


Figure 4. Performance of the coded and uncoded alternative JTIDS/Link-16 waveform for  $\rho = 0.2$  and  $E_b / N_0 = 9$  (dB) .

The performance of 32-BOK with (31,15) RS coding in PNI for different values of  $\rho$  with  $E_b / N_0 = 6$  dB is shown in Figure 5. Taking  $P_b = 10^{-5}$  as a reference, we compare the required  $E_b / N_I$  for different values of  $\rho$ . We see that when  $\rho = 1$ , which corresponds to barrage noise interference, the performance is better ( $E_b / N_I \approx 11$  dB) as compared to  $\rho = 0.2$  and  $\rho = 0.1$  ( $E_b / N_I \approx 12$  dB). The difference in performance between  $\rho = 0.2$  and  $\rho = 0.1$  is relatively small. From the figure, we see that between  $\rho = 1$  and  $\rho = 0.2$ , the transition point for which  $\rho = 1$  provides better performance occurs at  $P_b = 10^{-3}$  where  $E_b / N_I = 7.8$  dB. Note that the degradation due to PNI is only about 1 dB at  $P_b = 10^{-5}$ .

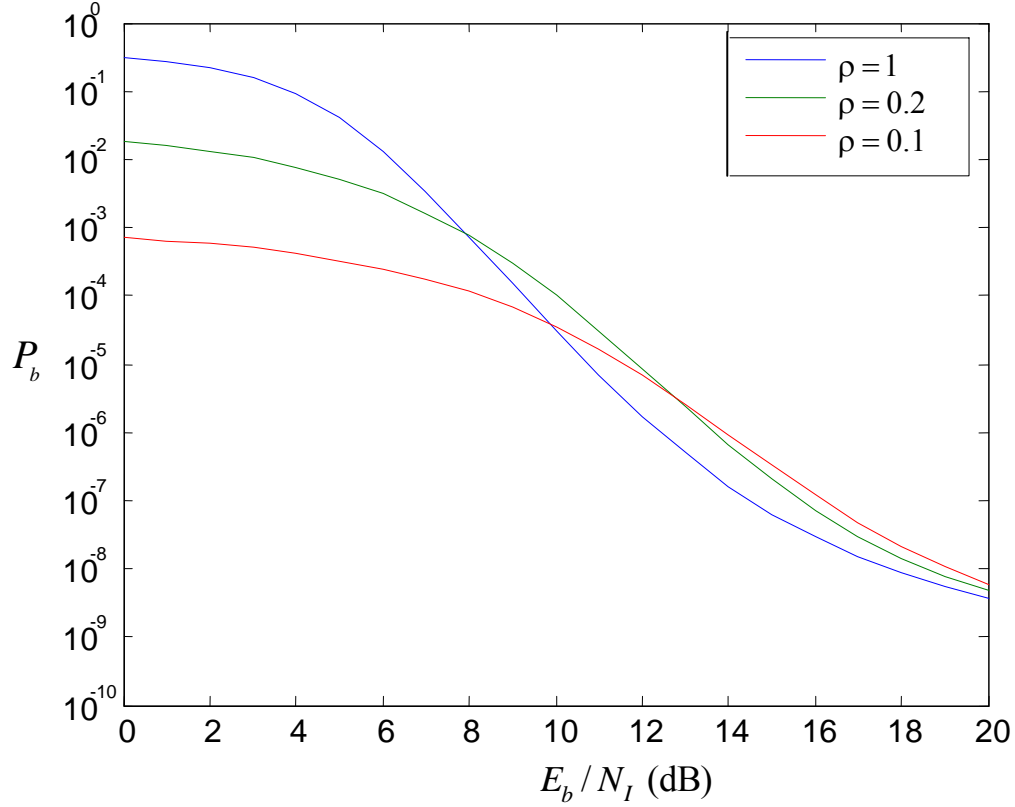


Figure 5. Performance of 32-BOK with (31,15) RS coding in PNI with  $E_b/N_0 = 6$  dB for different values of  $\rho$ .

The performance of 32-BOK with (31,15) RS coding in PNI for different values of  $\rho$  with  $E_b/N_0 = 9$  dB is plotted in Figure 6. As expected, when  $E_b/N_0$  increases, we see an improvement in overall performance; smaller values of  $E_b/N_I$  are required for the same  $P_b$ . In this case, when  $P_b = 10^{-5}$ ,  $E_b/N_I = 6.8$  dB is required for  $\rho = 1$  and  $E_b/N_I = 9.4$  dB is required for  $\rho = 0.2$ . This compares with  $E_b/N_I = 11$  dB for  $\rho = 1$  and  $E_b/N_I = 12$  dB for  $\rho = 0.2$  at  $P_b = 10^{-5}$  when  $E_b/N_0 = 6$  dB (Figure 5). This corresponds to a degradation of 2.6 dB ( $E_b/N_0 = 9$  dB) and 1 dB ( $E_b/N_0 = 6$  dB) due to PNI. Thus, while the absolute performance due to PNI improves as  $E_b/N_0$  increases, relative degradation also increases.

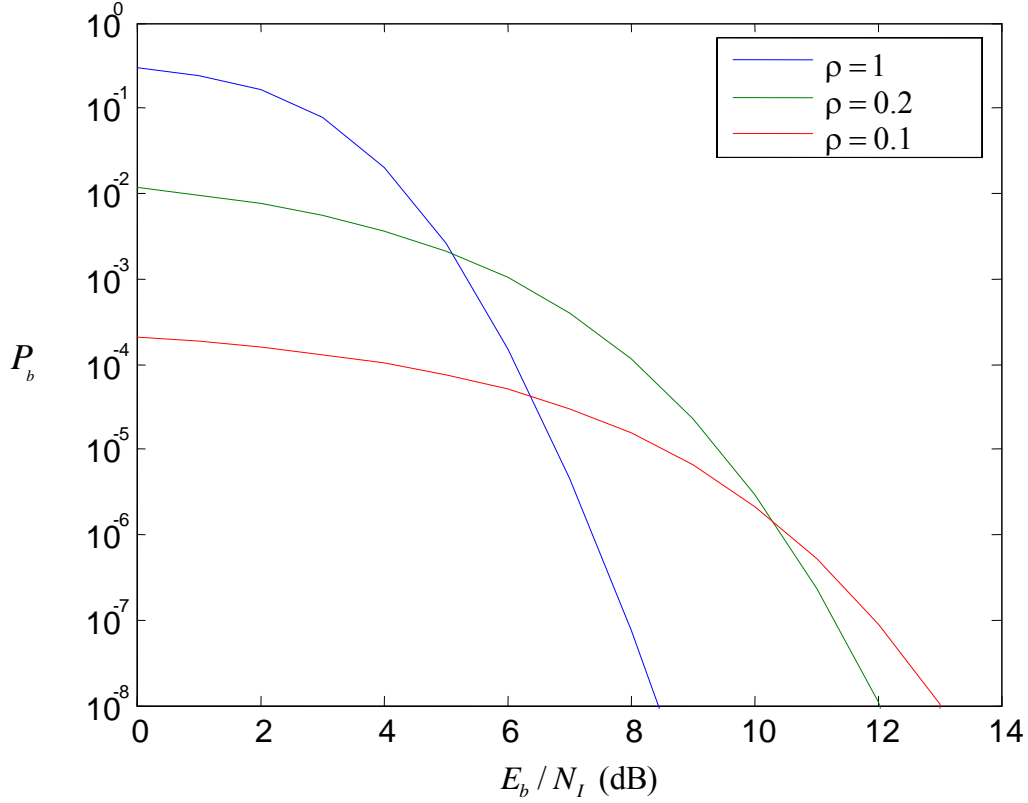


Figure 6. Performance of 32-BOK with (31,15) RS coding in PNI with  $E_b / N_0 = 9$  dB for different values of  $\rho$ .

### C. PERFORMANCE WITH ERRORS-AND-ERASURES DECODING IN AWGN

At the MBOK demodulator, the receiver has to decide which of the  $M$  symbols was received or decide that it cannot make a decision with sufficient confidence. If the output of each integrator,  $V_T > X_i > -V_T$ ,  $i = 1, 2, \dots, M/2$ , then the receiver cannot decide with sufficient confidence, and the symbol is erased.

Without loss of generality, we assume that the original signal representing symbol ‘1’ is transmitted. With errors-and-erasures, if symbol ‘1’ is transmitted, then the probability of channel symbol erasure  $p_e$  and probability of correct symbol detection  $p_c$  are [9]

$$p_e = \Pr(V_T > X_1 > -V_T \cap V_T > X_2 > -V_T \cap \dots \cap V_T > X_{M/2} > -V_T | 1) \quad (3.8)$$

and

$$p_c = \Pr(X_1 > V_T \cap |X_1| > |X_2| \cap |X_1| > |X_3| \cap \dots \cap |X_1| > |X_{M/2}| | 1), \quad (3.9)$$

respectively.

The probability of channel symbol error can be obtained by substituting (3.8) and (3.9) into (2.21).

From (3.8), when the output of each integrator  $V_T > X_i > -V_T$ ,  $i = 1, 2, \dots, M/2$ , the receiver cannot decide with sufficient confidence, and the symbol is erased. Hence the probability of symbol erasure is given by

$$p_e = \int_{-V_T}^{V_T} \int_{-V_T}^{V_T} \int_{-V_T}^{V_T} \dots \int_{-V_T}^{V_T} f_{X_1 X_2 \dots X_{M/2}}(x_1, x_2, \dots, x_{M/2} | 1) dx_1 dx_2 dx_3 \dots dx_{M/2} \quad (3.10)$$

where  $f_{X_1 X_2 \dots X_{M/2}}(x_1, x_2, \dots, x_{M/2} | 1)$  represents the joint probability density function of the random variables that model the detector outputs. Since the random variables that model the detector outputs are independent, (3.10) can be written as

$$\begin{aligned} p_e &= \int_{-V_T}^{V_T} f_{X_1}(x_1 | 1) dx_1 \int_{-V_T}^{V_T} f_{X_2}(x_2 | 1) dx_2 \\ &\quad \times \int_{-V_T}^{V_T} f_{X_3}(x_3 | 1) dx_3 \dots \int_{-V_T}^{V_T} f_{X_{M/2}}(x_{M/2} | 1) dx_{M/2} \end{aligned} \quad (3.11)$$

Since  $\int_{-V_T}^{V_T} f_{X_2}(x_2 | 1) dx_2 = \int_{-V_T}^{V_T} f_{X_3}(x_3 | 1) dx_3 = \dots = \int_{-V_T}^{V_T} f_{X_{M/2}}(x_{M/2} | 1) dx_{M/2}$ ,

(3.11) simplifies to

$$p_e = \left[ \int_{-V_T}^{V_T} f_{X_1}(x_1 | 1) dx_1 \right] \left[ \int_{-V_T}^{V_T} f_{X_2}(x_2 | 1) dx_2 \right]^{M/2-1} \quad (3.12)$$

Substituting (2.2), (2.3), and (2.4) into (3.12), we obtain

$$p_e = \left[ \int_{-V_T}^{V_T} \frac{1}{\sqrt{2\pi}\sigma} \exp \left[ \frac{-(x_1 - \sqrt{2}A_c)^2}{2\sigma^2} \right] dx_1 \right] \left[ \int_0^{V_T} \frac{1}{\sqrt{2\pi}\sigma} \exp \left[ \frac{-x_2^2}{2\sigma^2} \right] dx_2 \right]^{M/2-1} \quad (3.13)$$

which can be evaluated to obtain

$$p_e = \left[ 1 - Q\left(\frac{V_T + \sqrt{2}A_c}{\sigma}\right) - Q\left(\frac{V_T - \sqrt{2}A_c}{\sigma}\right) \right] \left[ 1 - 2Q\left(\frac{V_T}{\sigma}\right) \right]^{M/2-1} \quad (3.14)$$

Alternatively, (3.14) can be written as

$$p_e = \left[ Q\left(\frac{\sqrt{2}A_c - V_T}{\sigma}\right) - Q\left(\frac{V_T + \sqrt{2}A_c}{\sigma}\right) \right] \left[ 1 - 2Q\left(\frac{V_T}{\sigma}\right) \right]^{M/2-1} \quad (3.15)$$

Defining  $V_T = a\sqrt{2}A_c$  where  $0 < a < 1$  and  $\sigma^2 = N_o / T_s$ , we get

$$p_e = \left[ Q\left(\frac{\sqrt{2}A_c - a\sqrt{2}A_c}{\sigma}\right) - Q\left(\frac{\sqrt{2}A_c + a\sqrt{2}A_c}{\sigma}\right) \right] \left[ 1 - 2Q\left(\frac{a\sqrt{2}A_c}{\sigma}\right) \right]^{M/2-1} \quad (3.16)$$

Hence,

$$p_e = \left[ Q\left((1-a)\sqrt{\frac{2E_s}{N_o}}\right) - Q\left((1+a)\sqrt{\frac{2E_s}{N_o}}\right) \right] \left[ 1 - 2Q\left(a\sqrt{\frac{2E_s}{N_o}}\right) \right]^{M/2-1} \quad (3.17)$$

From (3.17), the probability of channel erasure with  $(n, k)$  RS coding with code rate  $r$  is

$$p_e = \left[ Q\left((1-a)\sqrt{\frac{2rE_s}{N_o}}\right) - Q\left((1+a)\sqrt{\frac{2rE_s}{N_o}}\right) \right] \left[ 1 - 2Q\left(a\sqrt{\frac{2rE_s}{N_o}}\right) \right]^{M/2-1} \quad (3.18)$$

In terms of  $E_b / N_o$ , (3.18) can be expressed as

$$p_e = \left[ Q\left((1-a)\sqrt{\frac{2rmE_b}{N_o}}\right) - Q\left((1+a)\sqrt{\frac{2rmE_b}{N_o}}\right) \right] \left[ 1 - 2Q\left(a\sqrt{\frac{2rmE_b}{N_o}}\right) \right]^{M/2-1} \quad (3.19)$$

Next, we derive an expression for the probability of correct symbol detection from (3.9). From (3.9), we have

$$p_c = \int_{V_T}^{\infty} \left[ \int_{-x_1}^{x_1} \int_{-x_1}^{x_1} \dots \int_{x_1}^{x_1} f_{X_1 X_2 \dots X_{M/2}}(x_1, x_2, \dots, x_{M/2} | 1) dx_2 dx_3 \dots dx_{M/2} \right] dx_1 \quad (3.20)$$

and

$$p_c = \int_{V_T}^{\infty} f_{X_1}(x_1 | 1) \times \left[ \int_{-x_1}^{x_1} f_{X_2}(X_2 | 1) dx_2 \int_{-x_1}^{x_1} f_{X_3}(x_3 | 1) dx_3 \dots \int_{x_1}^{x_1} f_{X_{M/2}}(x_{M/2} | 1) dx_{M/2} \right] dx_1 \quad (3.21)$$

which simplifies to

$$p_c = \int_{V_T}^{\infty} f_{X_1}(x_1 | 1) \left[ \int_{-x_1}^{x_1} f_{X_2}(x_2 | 1) dx_2 \right]^{M/2-1} dx_1 \quad (3.22)$$

Substituting (2.2), (2.3) and (2.4) into (3.22), we get

$$p_c = \int_{-V_T}^{\infty} \frac{1}{\sqrt{2\pi}\sigma} \exp \left[ \frac{-(x_1 - \sqrt{2}A_c)^2}{2\sigma^2} \right] \left[ \int_{-x_1}^{x_1} \frac{1}{\sqrt{2\pi}\sigma} \exp \left( \frac{-x_2^2}{2\sigma^2} \right) dx_2 \right]^{M/2-1} dx_1 \quad (3.23)$$

which can be partially evaluated to obtain

$$p_c = \int_{V_T}^{\infty} \frac{1}{\sqrt{2\pi}\sigma} \exp \left[ \frac{-(x_1 - \sqrt{2}A_c)^2}{2\sigma^2} \right] \left[ 1 - 2Q \left( \frac{x_1}{\sigma} \right) \right]^{M/2-1} dx_1 \quad (3.24)$$

Letting  $u = (x_1 - \sqrt{2}A_c) / \sigma$  in (3.24), we get

$$p_c = \int_{\frac{V_T - \sqrt{2}A_c}{\sigma}}^{\infty} \frac{1}{\sqrt{2\pi}} e^{-\frac{u^2}{2}} \left[ 1 - 2Q \left( u + \frac{\sqrt{2}A_c}{\sigma} \right) \right]^{M/2-1} du \quad (3.25)$$

Now, with  $V_T = a\sqrt{2}A_c$  and  $\sigma = N_o / T_s$  as previously, we obtain the probability of correct channel detection for MBOK from (3.25) as

$$p_c = \frac{1}{\sqrt{2\pi}} \int_{-(1-a)\sqrt{\frac{2E_s}{N_o}}}^{\infty} e^{-\frac{u^2}{2}} \left[ 1 - 2Q \left( u + \sqrt{\frac{2E_s}{N_o}} \right) \right]^{M/2-1} du \quad (3.26)$$

From (3.26), the probability of correct channel detection for MBOK with FEC coding, expressed in terms of  $E_b / N_o$ , is

$$p_c = \frac{1}{\sqrt{2\pi}} \int_{-(1-a)\sqrt{\frac{2rmE_b}{N_o}}}^{\infty} e^{-\frac{u^2}{2}} \left[ 1 - 2Q \left( u + \sqrt{\frac{2rmE_b}{N_o}} \right) \right]^{M/2-1} du \quad (3.27)$$



Substituting (3.19) and (3.27) into (2.21), we obtain the probability of channel symbol error for MBOK with EED. The probability of block error is obtained by substituting (3.19), (3.27) and the results for  $p_s$  into (2.24), repeated here:

$$P_E = 1 - \left[ \sum_{i=0}^t \binom{n}{i} p_s^i \sum_{j=0}^{d_{\min}-1-2i} \binom{n-i}{j} p_e^j p_c^{n-i-j} \right] \quad (3.28)$$

Consequently, we can obtain the probability of symbol error and the probability of bit error for MBOK with  $(n, k)$  RS coding and EED in the presence of AWGN using (2.25) and (2.16), respectively.

The performance for 32-BOK with a (31,15) RS code and EED in AWGN for different values of  $a$  is shown in Figure 7. From the Figure, we see that performance degrades for large values of  $a$  ( $a \geq 0.8$ ). There is not much difference in performance for values of  $a$  less than 0.6.

Since  $a=0$  implies no EED, we conclude that there is no improvement in performance using EED for the alternative JTIDS/Link-16 waveform in the presence of AWGN. Instead, if  $a$  is too large, it degrades performance.

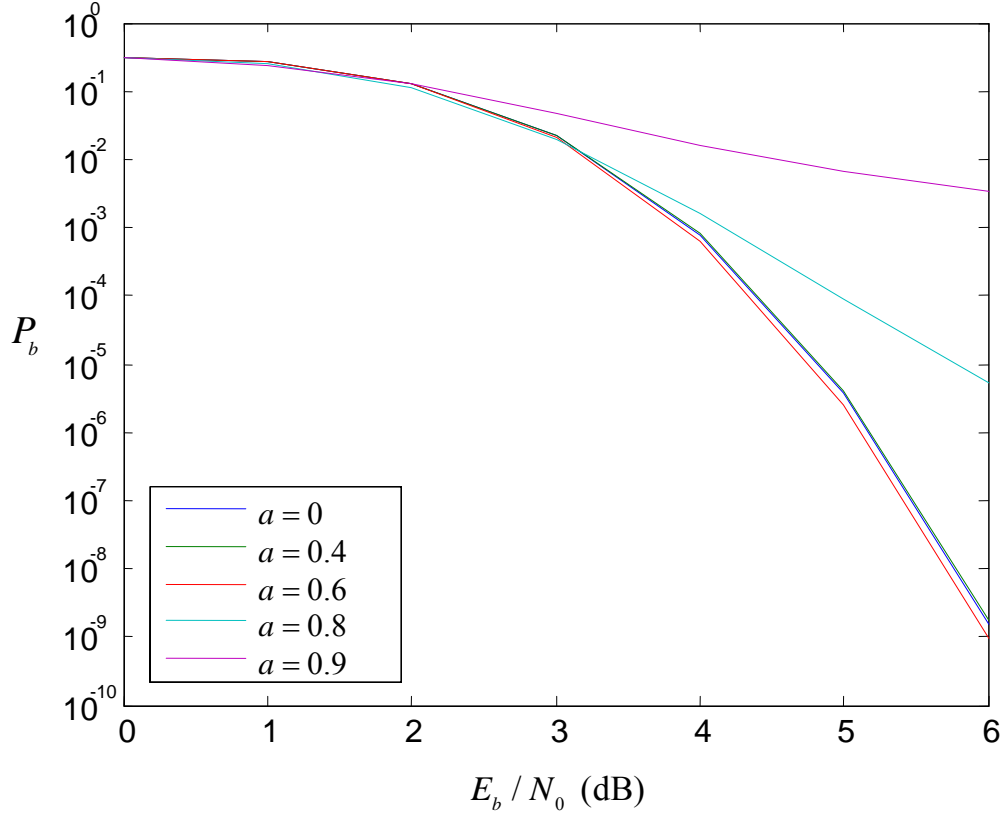


Figure 7. Performance of 32-BOK with (31,15) RS coding and EED for different values of  $a$  in the presence of AWGN.

#### D. PERFORMANCE WITH ERRORS-AND-ERASURES DECODING IN AWGN AND PULSE-NOISE INTERFERENCE

The probability of channel erasure with FEC and EED in the presence of PNI can be determined from (2.6), (2.8) and (3.16) in terms of  $E_b$  as

$$\begin{aligned}
p_e = & (1-\rho) \left[ Q \left( (1-a) \sqrt{\frac{2rmE_b}{N_o}} \right) - Q \left( (1+a) \sqrt{\frac{2rmE_b}{N_o}} \right) \right] \left[ 1 - 2Q \left( a \sqrt{\frac{2rmE_b}{N_o}} \right) \right]^{\frac{M}{2}-1} \\
& + (\rho) \left[ Q \left( (1-a) \sqrt{\frac{2rmE_b}{\frac{1}{\rho}N_I + N_o}} \right) - Q \left( (1+a) \sqrt{\frac{2rmE_b}{\frac{1}{\rho}N_I + N_o}} \right) \right] \\
& \times \left[ 1 - 2Q \left( a \sqrt{\frac{2rmE_b}{\frac{1}{\rho}N_I + N_o}} \right) \right]^{\frac{M}{2}-1}
\end{aligned} \tag{3.29}$$

As in (3.7), we express (3.29) in terms of  $\zeta$  and  $\gamma_b$  to get

$$\begin{aligned}
p_e = & (1-\rho) \left[ Q \left( (1-a) \sqrt{2rm\gamma_b} \right) - Q \left( (1+a) \sqrt{2rm\gamma_b} \right) \right] \left[ 1 - 2Q \left( a \sqrt{2rm\gamma_b} \right) \right]^{\frac{M}{2}-1} \\
& + (\rho) \left[ Q \left( (1-a) \sqrt{2rm\zeta} \right) - Q \left( (1+a) \sqrt{2rm\zeta} \right) \right] \left[ 1 - 2Q \left( a \sqrt{2rm\zeta} \right) \right]^{\frac{M}{2}-1}
\end{aligned} \tag{3.30}$$

Similarly, we can also obtain the probability of correct channel detection from (2.6), (2.8) and (3.25) as either

$$\begin{aligned}
p_c = & (1-\rho) \left\{ \frac{1}{\sqrt{2\pi}} \int_{-(1-a)\sqrt{\frac{2rmE_b}{N_o}}}^{\infty} e^{-\frac{u^2}{2}} \left[ 1 - 2Q \left( u + \sqrt{\frac{2rmE_b}{N_o}} \right) \right]^{\frac{M}{2}-1} du \right\} \\
& + \rho \left\{ \frac{1}{\sqrt{2\pi}} \int_{-(1-a)\sqrt{\frac{2rmE_b}{\frac{1}{\rho}N_I + N_o}}}^{\infty} e^{-\frac{u^2}{2}} \left[ 1 - 2Q \left( u + \sqrt{\frac{2rmE_b}{\frac{1}{\rho}N_I + N_o}} \right) \right]^{\frac{M}{2}-1} du \right\}
\end{aligned} \tag{3.31}$$

or

$$\begin{aligned}
p_c = & (1-\rho) \left\{ \frac{1}{\sqrt{2\pi}} \int_{-(1-a)\sqrt{2rm\gamma_b}}^{\infty} e^{-\frac{u^2}{2}} \left[ 1 - 2Q \left( u + \sqrt{2rm\gamma_b} \right) \right]^{\frac{M}{2}-1} du \right\} \\
& + \rho \left\{ \frac{1}{\sqrt{2\pi}} \int_{-(1-a)\sqrt{2rm\zeta}}^{\infty} e^{-\frac{u^2}{2}} \left[ 1 - 2Q \left( u + \sqrt{2rm\zeta} \right) \right]^{\frac{M}{2}-1} du \right\}
\end{aligned} \tag{3.32}$$

Substituting (3.32) and (3.30) into (2.21), we obtain the probability of channel symbol with EED.

Consequently, we can obtain the probability of block error by substituting (2.21), (3.30) and (3.32) into (2.24). The average probability of symbol error as well as the probability of bit error is obtained from the probability of block error by taking the average of their upper bound and lower bound as expressed in (2.25) and (2.16), respectively.

The performance of 32-BOK with (31,15) RS coding for different values of  $a$  where  $\rho = 1$  ( $E_b / N_0 = 6$  dB) in the presence of AWGN and PNI is shown in Figure 8. We observe  $a = 0.2$  and  $a = 0.4$  provide almost the same performance at  $P_b = 10^{-5}$ , while  $a = 0.6$  gives slightly better performance. The worst performance occurs for  $a = 0.8$ .

Next, we investigate the performance of the alternative waveform with EED for different  $\rho$  when  $a = 0.6$ .

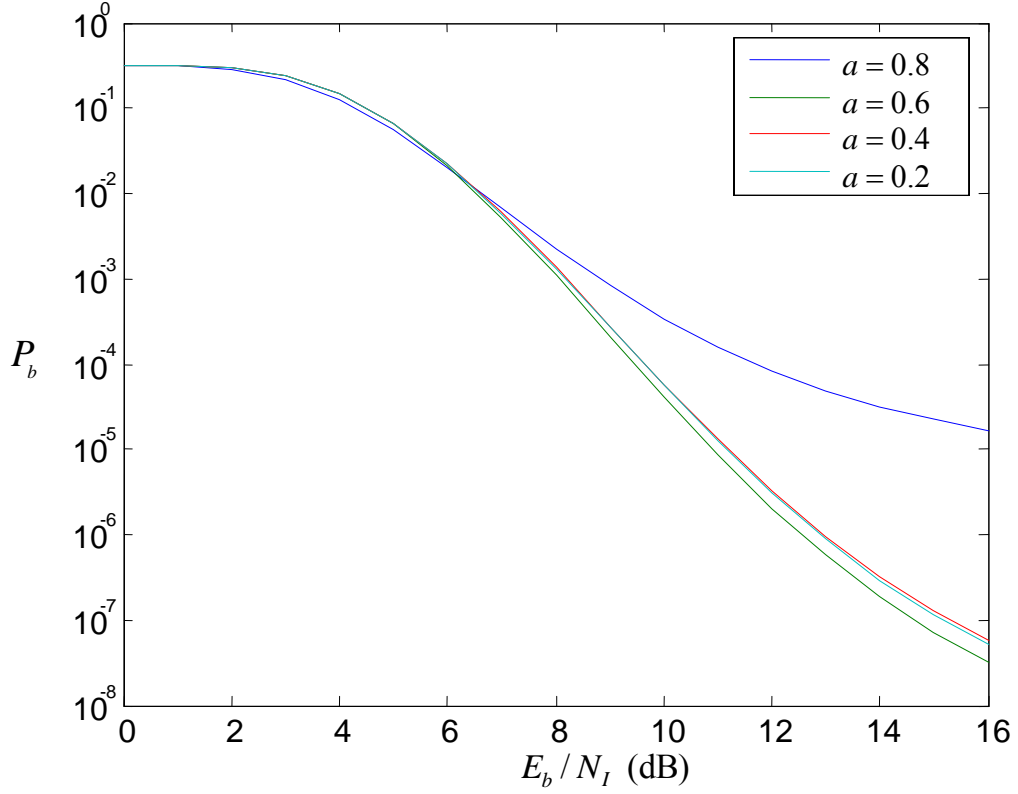


Figure 8. Performance of 32-BOK with (31,15) RS coding and EED for  $\rho = 1$  and  $E_b/N_0 = 6$  dB for different values of  $a$ .

The performance of 32-BOK with (31,15) RS coding with EED in a PNI environment for various values of  $\rho$  with  $a = 0.6$  and  $E_b/N_0 = 6$  dB is shown in Figure 9. We observe that at  $P_b = 10^{-5}$ , as  $\rho$  decreases, performance is degraded, but the degradation is limited to about 2 dB.

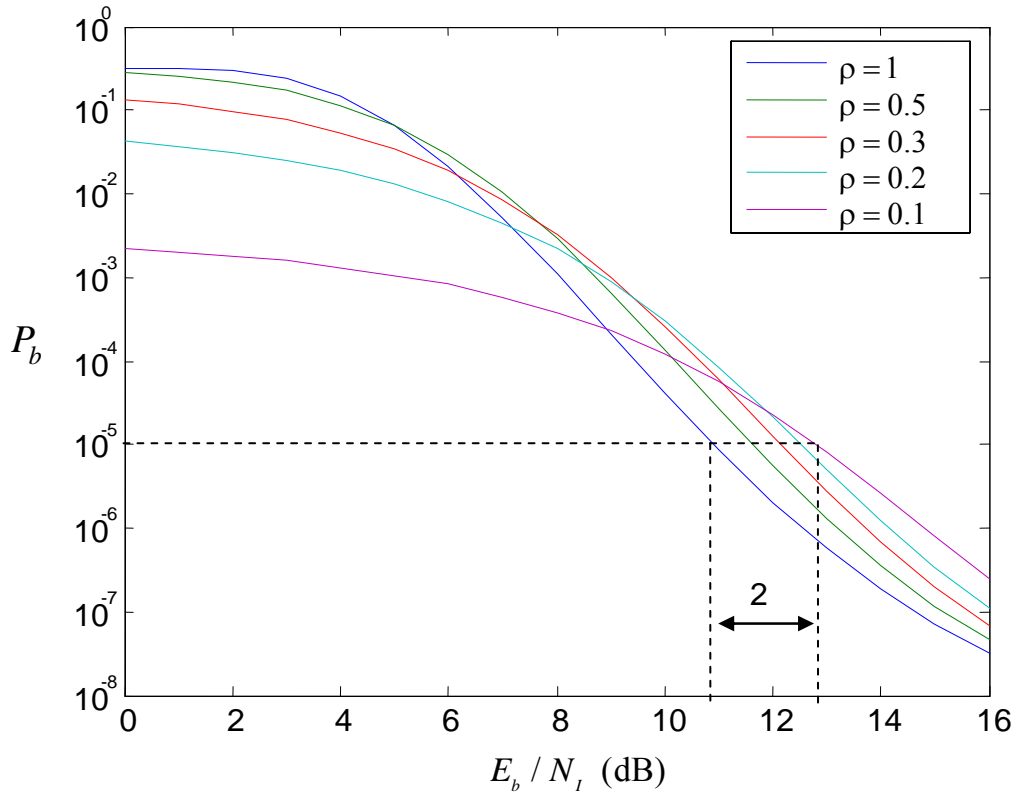


Figure 9. Performance of 32-BOK with (31,15) RS coding with EED in a PNI environment for  $a = 0.6$  and  $E_b / N_0 = 6$  dB.

The performance for 32-BOK with (31,15) RS coding both with and without EED for  $E_b / N_0 = 6$  dB and different values of  $\rho$  in the presence of AWGN and PNI is shown in Figure 10. At  $P_b = 10^{-5}$ , when  $\rho = 0.2$  or  $0.1$ , there is no improvement due to EED but a degradation of 0.1 to 0.5 dB. The only exception is when  $\rho = 1$ , where we see that using EED performs slightly better, of 0.2 dB, than without EED.

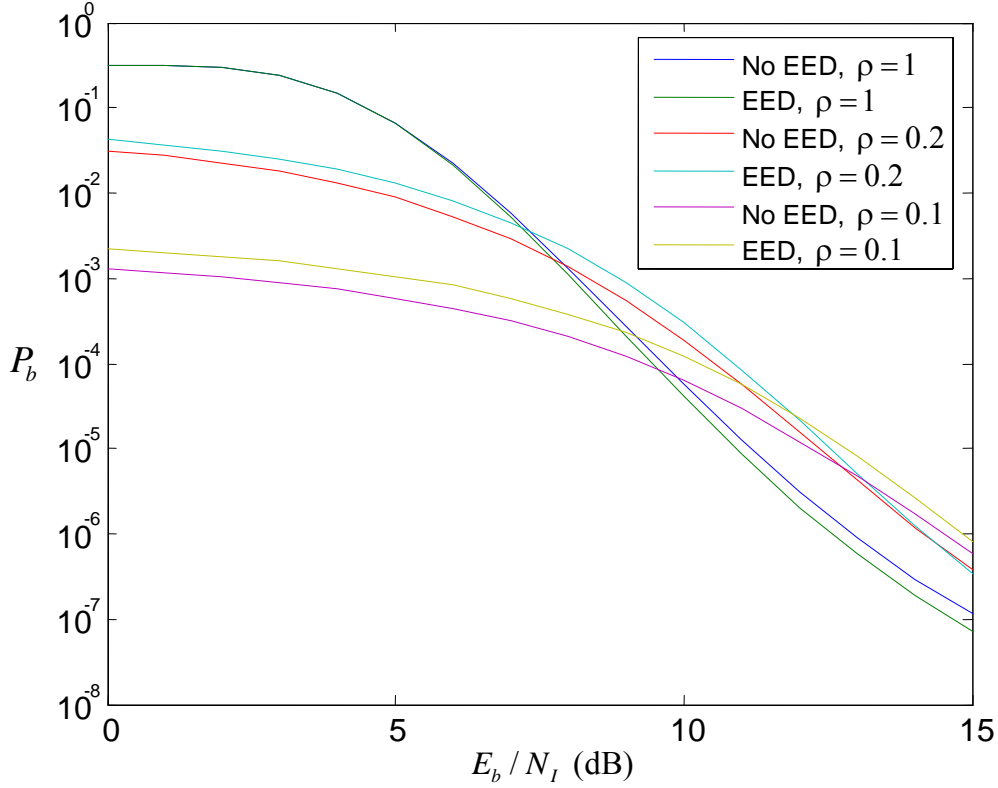


Figure 10. Performance of 32-BOK with RS coding with and without EED with  $E_b / N_0 = 6$  dB and  $a = 0.6$  for different  $\rho$ .

Figure 11 is similar to Figure 10 except  $a = 0.4$ . In this case, there is no difference in performance for different values of  $\rho$  with or without EED.

We conclude that 32-BOK with (31,15) RS coding with EED does not significantly improve the performance of the waveform and may instead degrade performance for  $\rho < 1$ . This results is somewhat surprising since EED has been shown to significantly reduce degradation due to PNI for waveforms with binary modulation and binary coding [13].

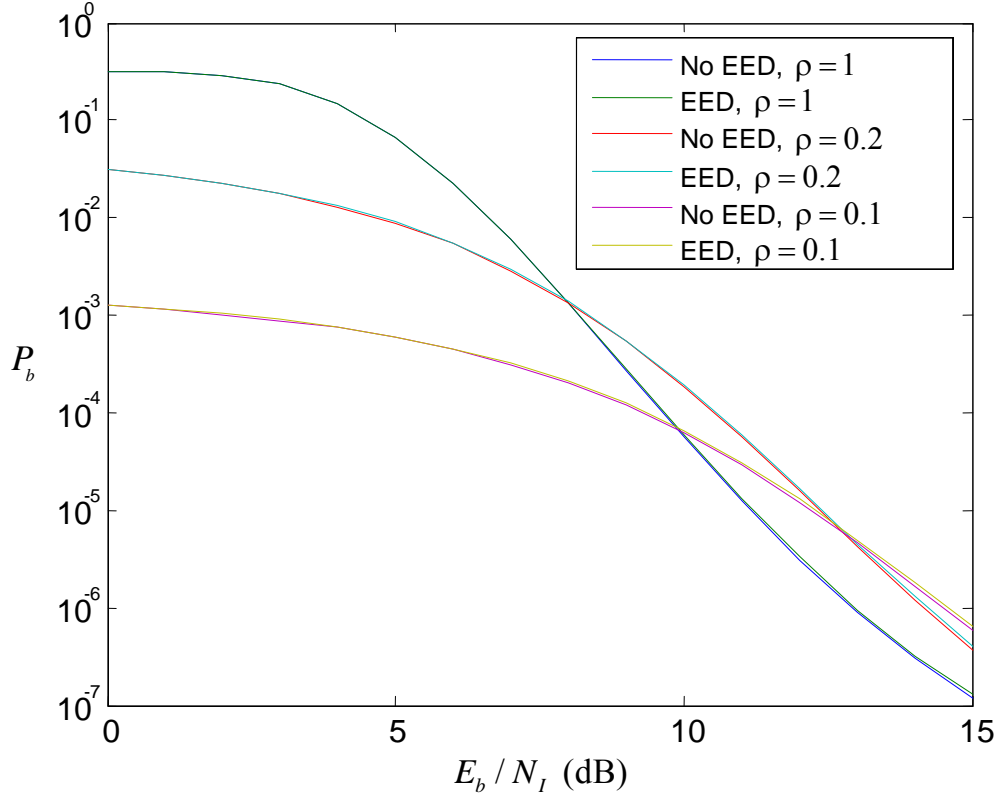


Figure 11. Performance of 32-BOK with (31,15) RS coding with and without EED with  $E_b/N_0 = 6$  dB and  $a = 0.4$  for different values of  $\rho$ .

## E. CHAPTER SUMMARY

In this chapter, the performance of the alternative JTIDS/Link-16 waveform with no diversity (single-pulse structure) was investigated both with and without EED and for AWGN only as well as AWGN plus PNI. We saw that the waveform performs better in barrage noise interference than PNI. We also see that EED decoding does not substantially improve performance for the receiver when both AWGN and PNI are present. In Chapter IV, we investigate the performance of the alternative JTIDS/Link-16 waveform with a diversity of two (double-pulse structure).



## IV. PERFORMANCE OF THE ALTERNATIVE JTIDS/LINK-16 WAVEFORM WITH DIVERSITY TWO (DOUBLE-PULSE STRUCTURE)

In this chapter, we investigate the performance of the alternative JTIDS/Link-16 waveform with a diversity of two (double-pulse structure). Diversity is widely used when the channel is susceptible to PNI and/or fading. Diversity improves the performance of the system by providing transmission redundancy.

### A. PERFORMANCE IN AWGN WITH A DIVERSITY OF TWO

The probability of channel symbol error for MBOK is given in (2.5). As discussed earlier, JTIDS/Link-16 employs diversity in its pulse structure to obtain improved performance. The double-pulse structure improves the performance of the system while the single-pulse structure allows for higher throughput. In Chapter III, we analyzed the performance of the alternative JTIDS/Link-16 waveform based on the single-pulse structure. In this chapter, we investigate the performance of the alternative waveform for the double-pulse structure.

Since the received energy per bit is  $L$  times the average received energy per chip,  $E_b = LE_c$ , the modified expression for  $p_s$  with diversity can be obtained from (3.2). With the double-pulse structure, giving a diversity of two ( $L = 2$ ), the received energy per bit is the combination of two chip's energy, giving twice the energy per symbol received. Hence, the probability of channel symbol error for MBOK with  $(n, k)$  RS coding having a diversity of  $L$  in terms of chip energy is

$$p_s = 1 - \frac{1}{\sqrt{2\pi}} \int_{-\sqrt{2LrmE_c/N_0}}^{\infty} e^{-\frac{u^2}{2}} \left[ 1 - 2Q\left(u + \sqrt{\frac{2LrmE_c}{N_0}}\right) \right]^{\frac{M}{2}-1} du \quad (4.1)$$

where  $E_c$  is the average energy per chip and soft decision demodulation is assumed. Since  $L = 2$ , (4.1) simplifies to

$$p_s = 1 - \frac{1}{\sqrt{2\pi}} \int_{-\sqrt{4rmE_c/N_0}}^{\infty} e^{-\frac{u^2}{2}} \left[ 1 - 2Q\left(u + \sqrt{\frac{4rmE_c}{N_0}}\right) \right]^{\frac{M}{2}-1} du \quad (4.2)$$

We can obtain the probability of information symbol error and information bit error using (3.4) and (2.16), repeated here for convenience:

$$P_s \approx \frac{1}{n} \sum_{j=t+1}^n i \binom{n}{j} p_s^j (1-p_s)^{n-j} \quad (4.3)$$

$$P_b = \left( \frac{1+m}{2m} \right) P_s \quad (4.4)$$

By comparing (3.2) and (4.2), we see that diversity gives a 3 dB improvement in performance as compared to no diversity in terms of average energy per chip. The improvement is shown in Figure 12. The difference in the required  $E_c/N_0$  between the double-pulse and the single-pulse is 3 dB at  $P_b = 10^{-5}$  in AWGN.

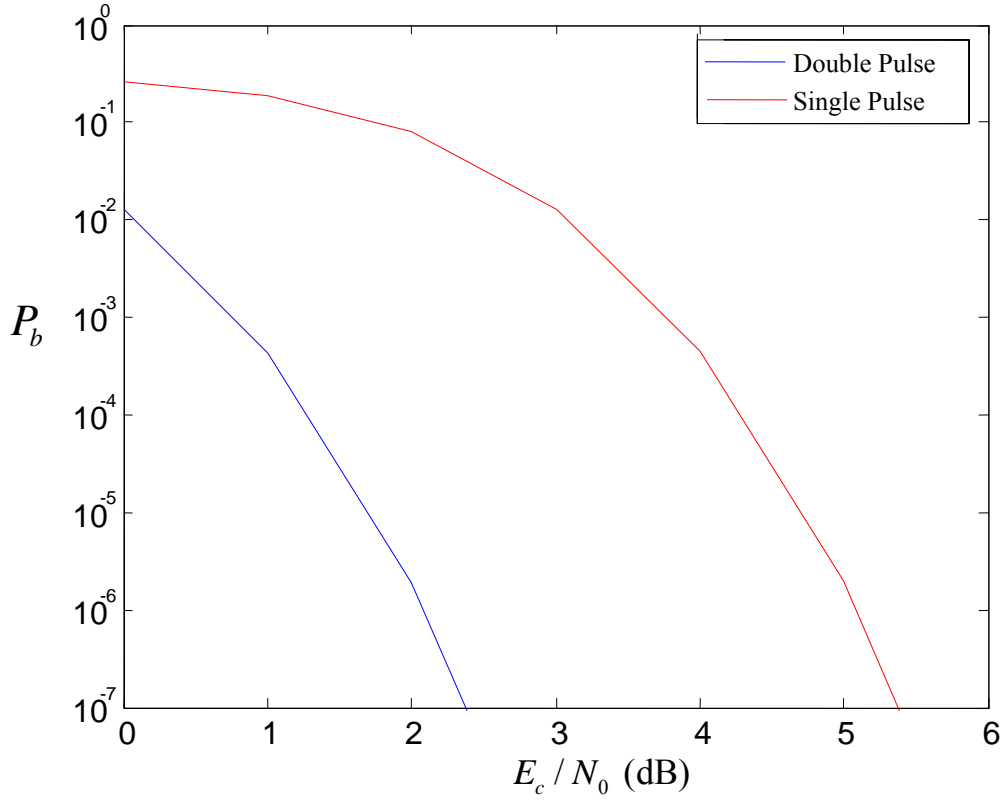


Figure 12. Performance of 32-BOK with (31,15) RS coding for both the single-pulse and the double-pulse structure in AWGN.

## B. PERFORMANCE IN AWGN AND PNI WITH A DIVERSITY OF TWO

For a channel with PNI in addition to AWGN, the probability of channel symbol error for a diversity of two is given by

$$p_s = \sum_{i=0}^2 \binom{2}{i} \rho^i (1-\rho)^{2-i} p_{chip}(i) \quad (4.5)$$

where  $p_{chip}(i)$  is the conditional probability of channel chip error given that  $i$  chips experience PNI.

The conditional probability density functions for the random variables  $X_m$ , where  $m=1,2,\dots,M/2$ , that represent the decision variables obtained by soft combining of the integrator outputs are given by

$$f_{X_m}(x_m | m, i) = \frac{1}{\sqrt{2\pi}\sigma_m(i)} \exp \left[ \frac{-(x_m - 2\sqrt{2}A_c)^2}{2\sigma_m^2(i)} \right] \quad \text{for } m \leq M/2, \quad (4.6)$$

$$f_{X_m}(x_m | m, i) = \frac{1}{\sqrt{2\pi}\sigma_m(i)} \exp \left[ \frac{-(x_m + 2\sqrt{2}A_c)^2}{2\sigma_m^2(i)} \right] \quad \text{for } M/2+1 \leq m \leq M, \quad (4.7)$$

and

$$f_{X_n}(x_n | n, n \neq m, i) = \frac{1}{\sqrt{2\pi}\sigma_m(i)} \exp \left[ \frac{-x_n^2}{2\sigma_m^2(i)} \right] \quad (4.8)$$

where

$$\sigma_m^2(i) = i\sigma_T^2 + (2-i)\sigma_0^2 \quad (4.9)$$

and

$$\sigma_T^2 = \sigma_I^2 + \sigma_0^2. \quad (4.10)$$

With  $\sigma_0^2 = N_0 / rT_s$  and  $\sigma_I^2 = N_I / \rho rT_s$ , and substituting (4.10) into (4.9), we have

$$\sigma_m^2(i) = i \frac{N_I}{\rho rT_s} + 2 \frac{N_0}{rT_s} \quad (4.11)$$

Comparing (4.6) — (4.11) to (2.2) — (2.4), we can adapt (2.5) to obtain the probability of channel chip error as

$$p_{chip}(i) = 1 - \int_0^\infty \frac{1}{\sqrt{2\pi}\sigma_m(i)} e^{-\frac{(x_1 - 2\sqrt{2}A_c)^2}{2\sigma_m^2(i)}} \left[ 1 - 2Q\left(\frac{x_1}{\sigma_m(i)}\right) \right]^{\frac{M}{2}-1} dx_1 \quad (4.12)$$

which can be expressed as

$$p_{chip}(i) = 1 - \frac{1}{\sqrt{2\pi}} \int_{-\sqrt{\frac{2E_s}{iN_I + 2N_0}}}^\infty e^{-\frac{u^2}{2}} \left[ 1 - 2Q\left(u + 2\sqrt{\frac{2E_s}{i\frac{N_I}{\rho} + 2N_0}}\right) \right]^{\frac{M}{2}-1} du \quad (4.13)$$

The conditional probability of channel chip error with coding and expressed in terms of chip energy is given by

$$p_{chip}(i) = 1 - \frac{1}{\sqrt{2\pi}} \int_{-\sqrt{\frac{2rmE_c}{iN_I + 2N_0}}}^\infty e^{-\frac{u^2}{2}} \left[ 1 - 2Q\left(u + 2\sqrt{\frac{2rmE_c}{i\frac{N_I}{\rho} + 2N_0}}\right) \right]^{\frac{M}{2}-1} du \quad (4.14)$$

which can be expressed by

$$p_{chip}(i) = 1 - \frac{1}{\sqrt{2\pi}} \int_{-\sqrt{\frac{2rm}{i\gamma_I^{-1} + 2\gamma_c^{-1}}}}^\infty e^{-\frac{u^2}{2}} \left[ 1 - 2Q\left(u + 2\sqrt{\frac{2rm}{i\gamma_I^{-1} + 2\gamma_c^{-1}}}\right) \right]^{\frac{M}{2}-1} du \quad (4.15)$$

where  $\gamma_I = E_c / N_I$ ,  $\gamma_c = E_c / N_0$ , and (4.15) is substituted into (4.5) to obtain the probability of channel symbol error. The probability of information symbol error for 32-BOK with (31,15) RS coding and a diversity of two is obtained by substituting (4.5) into (4.3).

The performance for different values of  $\rho$  with  $E_c / N_0 = 2.4$  dB is shown in Figure 13. The  $E_c / N_0$  is chosen to be 2.4 dB since this yields  $P_b = 10^{-7}$  at  $E_c / N_I = 25$  dB. We see that varying  $\rho$  does not degrade the performance of the receiver

significantly as compared to barrage jamming ( $\rho = 1$ ). At  $P_b = 10^{-5}$ , degradation due to PNI is only about 1 dB, and very small  $\rho$  ( $\rho = 0.02$ ) results in better performance as compared to larger  $\rho$ .

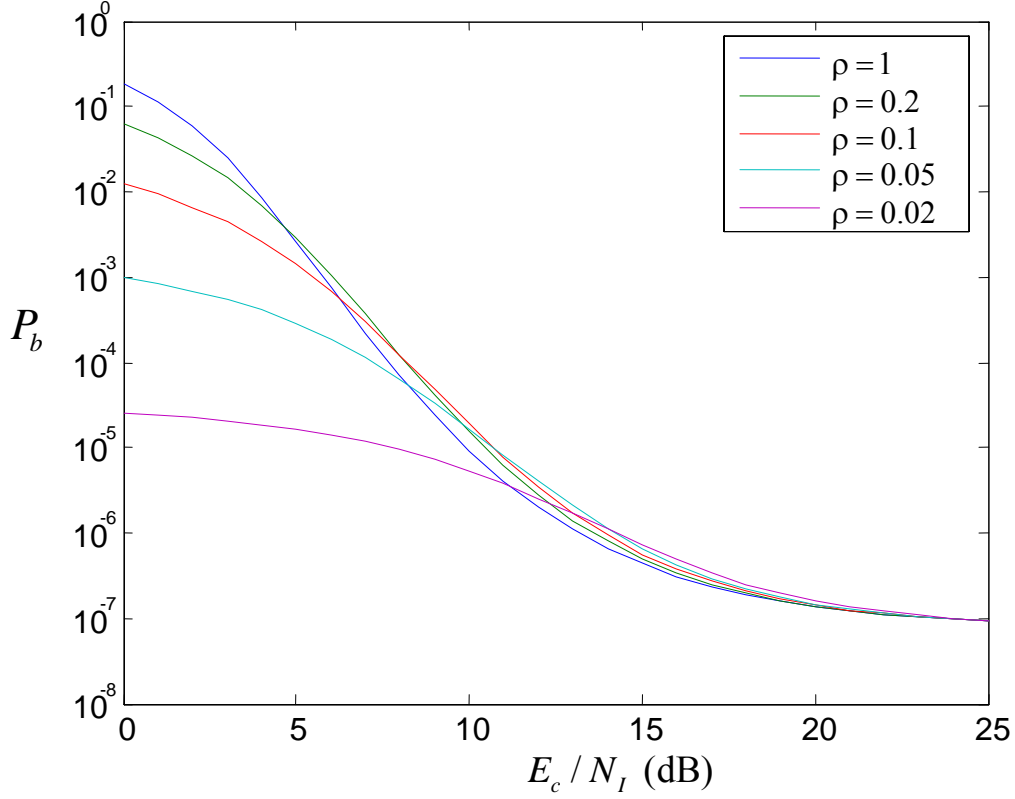


Figure 13. Performance of 32-BOK with (31,15) RS coding and the double-pulse structure for different  $\rho$  with  $E_c / N_0 = 2.4$  dB.

In Figure 14,  $E_c / N_0 = 3$  dB and performance approaches  $10^{-9}$  at  $E_c / N_I = 25$  dB. In this case, degradation due to PNI increases to about 2 dB, but absolute performance improves by about 2.5 dB.

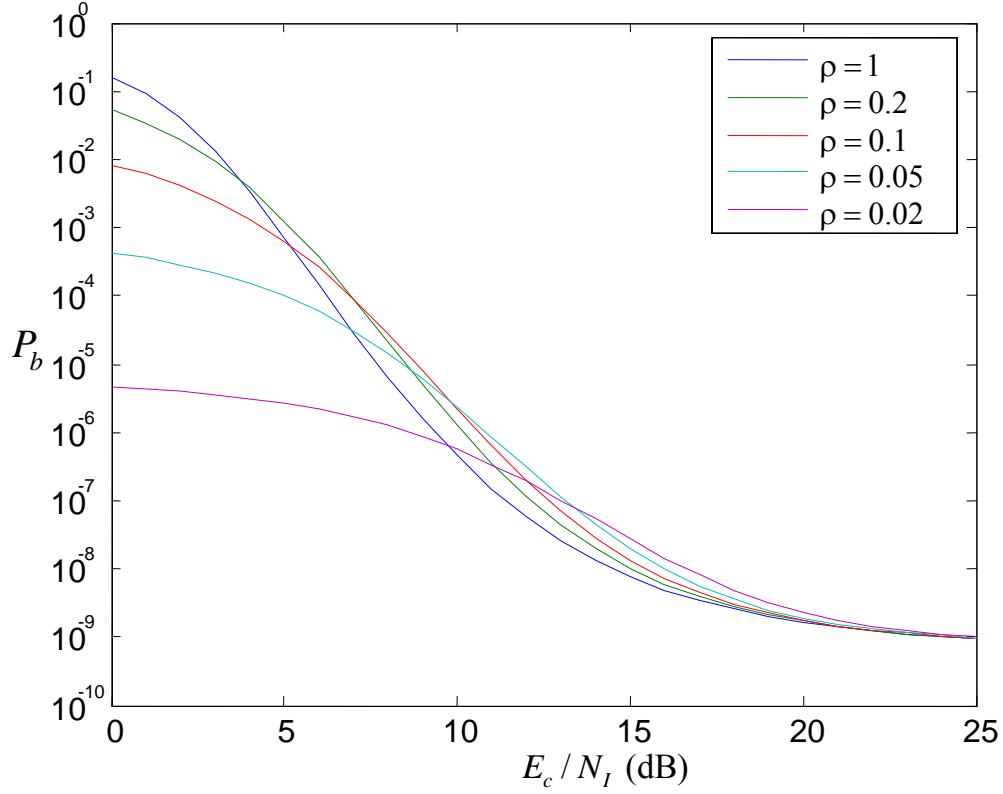


Figure 14. Performance of 32-BOK with (31,15) RS coding and the double-pulse structure for different  $\rho$  with  $E_c / N_0 = 3$  dB .

In Figure 15, we compare the performance for receivers both with and without diversity where the probability of bit error approaches  $E_c / N_t = 25$  dB . For the receiver without diversity,  $E_c / N_0 = 5.4$  dB for an asymptotic limit of  $10^{-7}$  while with diversity,  $E_c / N_0$  is 3 dB less. The difference in performance between the waveforms with and without diversity is about 3 dB for both  $\rho=1$  and 0.1 at  $P_b = 10^{-5}$  .

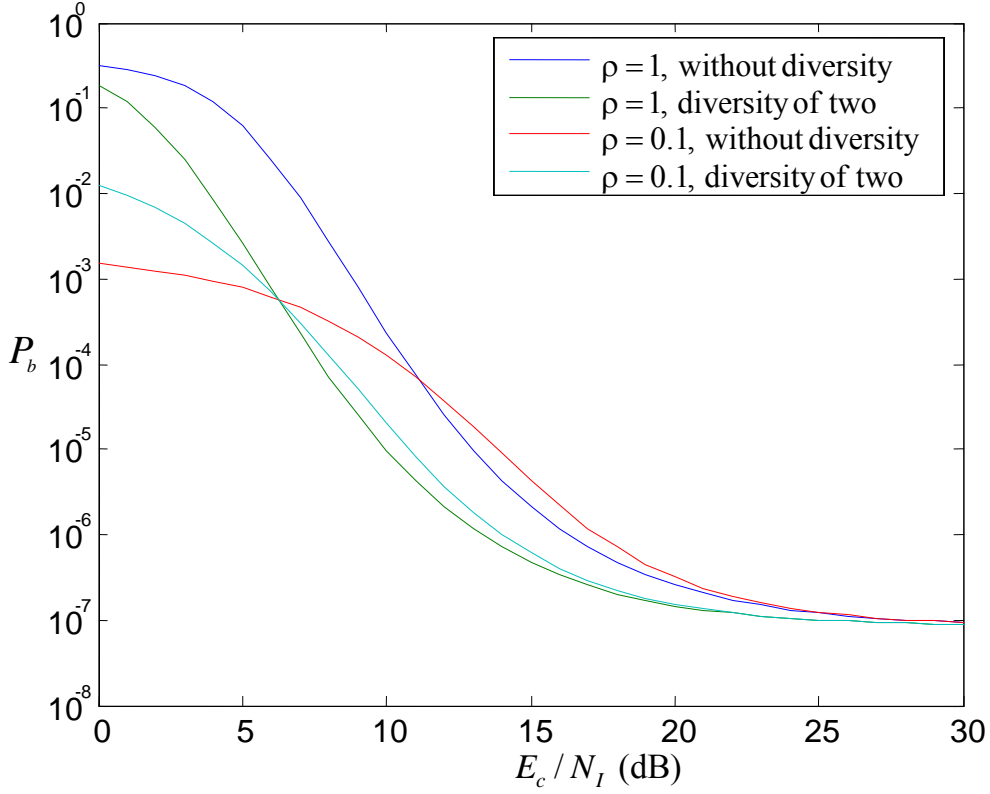


Figure 15. Performance of 32-BOK with (31,15) RS coding for both the double-pulse structure ( $E_c / N_0 = 2.4$  dB) and the single-pulse structure ( $E_b / N_0 = 5.4$  dB).

### C. PERFORMANCE IN AWGN AND PNI WITH A DIVERSITY OF TWO AND EED

The probability of bit error with EED can be obtained using similar approach as that with no diversity. We first obtain the probability of correct channel detection and the probability of channel erasure to obtain the probability of channel symbol error.

Recall from (3.12) that the probability of channel erasure is

$$p_e = \left[ \int_{-V_T}^{V_T} f_{X_1}(x_1 | 1) dx_1 \right] \left[ \int_{-V_T}^{V_T} f_{X_2}(x_2 | 1) dx_2 \right]^{M/2-1} \quad (4.16)$$

From (4.6), (4.7), (4.8) and (4.16), the conditional probability of channel erasure given that  $i$  diversity receptions experience PNI is

$$p_e(i) = \left[ \int_{-V_T}^{V_T} \frac{1}{\sqrt{2\pi}\sigma_m(i)} \exp\left[\frac{-(x_1 - 2\sqrt{2}A_c)^2}{2\sigma_m^2(i)}\right] dx_1 \right] \times \left[ 2 \int_0^{V_T} \frac{1}{\sqrt{2\pi}\sigma_m(i)} \exp\left[\frac{-x_2^2}{2\sigma_m^2(i)}\right] dx_2 \right]^{M/2-1} \quad (4.17)$$

which can be evaluated to obtain

$$p_e(i) = \left[ Q\left(\frac{2\sqrt{2}A_c - V_T}{\sigma_m(i)}\right) - Q\left(\frac{2\sqrt{2}A_c + V_T}{\sigma_m(i)}\right) \right] \left[ 1 - Q\left(\frac{V_T}{\sigma_m(i)}\right) \right]^{\frac{M}{2}-1} \quad (4.18)$$

Defining  $V_T = a(2\sqrt{2}A_c)$  where  $0 < a < 1$ , and with (4.11), we obtain

$$p_e(i) = \left[ Q\left((1-a)2\sqrt{\frac{2E_s}{iN_I + 2N_0}}\right) - Q\left((1+a)2\sqrt{\frac{2E_s}{iN_I + 2N_0}}\right) \right] \times \left[ 1 - 2Q\left(2a\sqrt{\frac{2E_s}{iN_I + 2N_0}}\right) \right]^{\frac{M}{2}-1} \quad (4.19)$$

which with coding can be expressed as

$$p_e(i) = \left[ Q\left((1-a)2\sqrt{\frac{2rmE_c}{\frac{i}{\rho}N_I + 2N_0}}\right) - Q\left((1+a)2\sqrt{\frac{2rmE_c}{\frac{i}{\rho}N_I + 2N_0}}\right) \right] \times \left[ 1 - 2Q\left(2a\sqrt{\frac{2rmE_c}{\frac{i}{\rho}N_I + 2N_0}}\right) \right]^{\frac{M}{2}-1} \quad (4.20)$$

where  $\rho$  represents the fraction of time the channel is affected by PNI,  $r$  is the code rate and  $E_c$  is the chip energy.



The probability of channel erasure for the double-pulse structure with EED is obtained by substituting (4.20) into (4.5):

$$\begin{aligned}
p_e = & \sum_{i=0}^2 \binom{2}{i} \rho^i (1-\rho)^{2-i} \\
& \times \left[ Q \left( (1-a) 2 \sqrt{\frac{2rmE_c}{\frac{i}{\rho} N_I + 2N_0}} \right) - Q \left( (1+a) 2 \sqrt{\frac{2rmE_c}{\frac{i}{\rho} N_I + 2N_0}} \right) \right] \\
& \times \left[ 1 - 2Q \left( 2a \sqrt{\frac{2rmE_c}{\frac{i}{\rho} N_I + 2N_0}} \right) \right]^{\frac{M}{2}-1}
\end{aligned} \tag{4.21}$$

Similarly, we can obtain the conditional probability of correct channel detection from (4.6), (4.7), (4.8) and (3.22) given that  $i$  diversity receptions experience PNI as

$$\begin{aligned}
p_c(i) = & \int_{-V_T}^{\infty} \frac{1}{\sqrt{2\pi}\sigma_m(i)} \exp \left[ \frac{-(x_1 - 2\sqrt{2}A_c)^2}{2\sigma_m^2(i)} \right] \\
& \times \left[ \int_{-x_1}^{x_1} \frac{1}{\sqrt{2\pi}\sigma_m(i)} \exp \left( \frac{-x_2^2}{2\sigma_m^2(i)} \right) dx_2 \right]^{M/2-1} dx_1
\end{aligned} \tag{4.22}$$

which can be partially evaluated to obtain

$$p_c(i) = \int_{V_T}^{\infty} \frac{1}{\sqrt{2\pi}\sigma_m(i)} \exp \left[ \frac{-(x_1 - 2\sqrt{2}A_c)^2}{2\sigma_m^2(i)} \right] \left[ 1 - 2Q \left( \frac{x_1}{\sigma_m(i)} \right) \right]^{M/2-1} dx_1 \tag{4.23}$$

Letting  $u = (x_1 - 2\sqrt{2}A_c) / \sigma_m(i)$  in (4.23), we get

$$p_c(i) = \int_{\frac{V_T - 2\sqrt{2}A_c}{\sigma_m(i)}}^{\infty} \frac{1}{\sqrt{2\pi}} e^{-\frac{u^2}{2}} \left[ 1 - 2Q \left( u + \frac{2\sqrt{2}A_c}{\sigma_m(i)} \right) \right]^{M/2-1} du \tag{4.24}$$

Now, with  $V_T = a(2\sqrt{2}A_c)$  and with (4.11), we obtain the conditional probability of correct channel detection for MBOK with FEC coding expressed in terms of  $E_c/N_o$  given that  $i$  diversity receptions experience PNI as

$$p_c(i) = \frac{1}{\sqrt{2\pi}} \int_{-(1-a)^2 \sqrt{\frac{2rmE_c}{\frac{iN_L}{\rho} + 2N_o}}}^{\infty} e^{-\frac{u^2}{2}} \left[ 1 - 2Q \left( u + 2 \sqrt{\frac{2rmE_c}{\frac{iN_L}{\rho} + 2N_o}} \right) \right]^{M/2-1} du \quad (4.25)$$

Substituting (4.25) into (4.5), we obtain the probability of correct channel detection for the double-pulse structure with EED as

$$p_e = \sum_{i=0}^2 \binom{2}{i} \rho^i (1-\rho)^{2-i} \times \frac{1}{\sqrt{2\pi}} \int_{-(1-a)^2 \sqrt{\frac{2rmE_c}{\frac{iN_L}{\rho} + 2N_o}}}^{\infty} e^{-\frac{u^2}{2}} \left[ 1 - 2Q \left( u + 2 \sqrt{\frac{2rmE_c}{\frac{iN_L}{\rho} + 2N_o}} \right) \right]^{M/2-1} du \quad (4.26)$$

Thus, we have the probability of channel symbol error with EED as

$$p_s = 1 - p_e - p_c \quad (4.27)$$

Using the results of  $p_e$ ,  $p_c$  and  $p_s$ , we obtain the probability of block error as

$$P_E = 1 - \left[ \sum_{i=0}^t \binom{n}{i} p_s^i \sum_{j=0}^{d_{\min}-1-2i} \binom{n-i}{j} p_e^j p_c^{n-i-j} \right] \quad (4.28)$$

and the probability of information symbol error and bit error can be obtained using (2.25) and (2.16), respectively.

The results for 32-BOK with (31,15) RS coding and EED and a diversity of two in PNI for different values of  $a$  are shown in Figure 16 and Figure 17 where  $E_c/N_o$  is

2.5 dB and 15 dB, respectively. We see that there is not much difference in performance for  $0.4 \leq a \leq 0.7$ . However, performance degrades for  $a > 0.7$ . This is expected since when  $a$  reaches a large value, many more received symbols are erased, overwhelming the erasure correction capability of the RS code. We use  $a = 0.6$  for subsequent analysis.

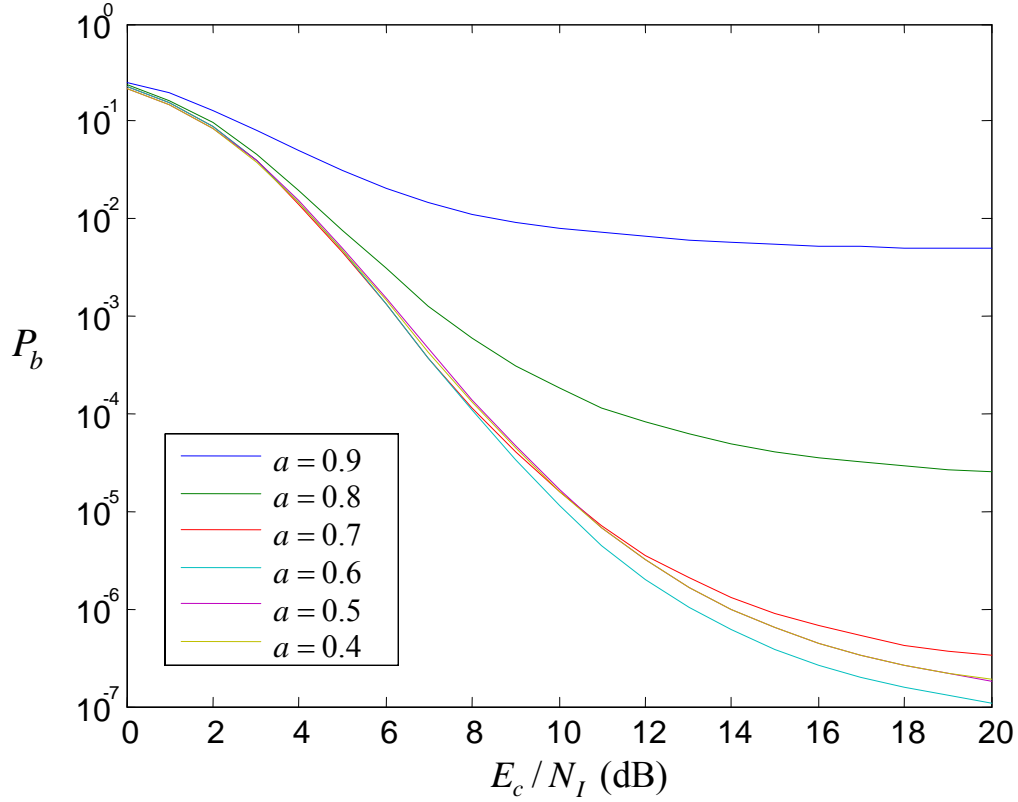


Figure 16. Performance of 32-BOK with (31,15) RS coding and EED for the double-pulse structure with  $\rho = 0.5$  and  $E_c / N_0 = 2.5$  dB for different values of  $a$ .

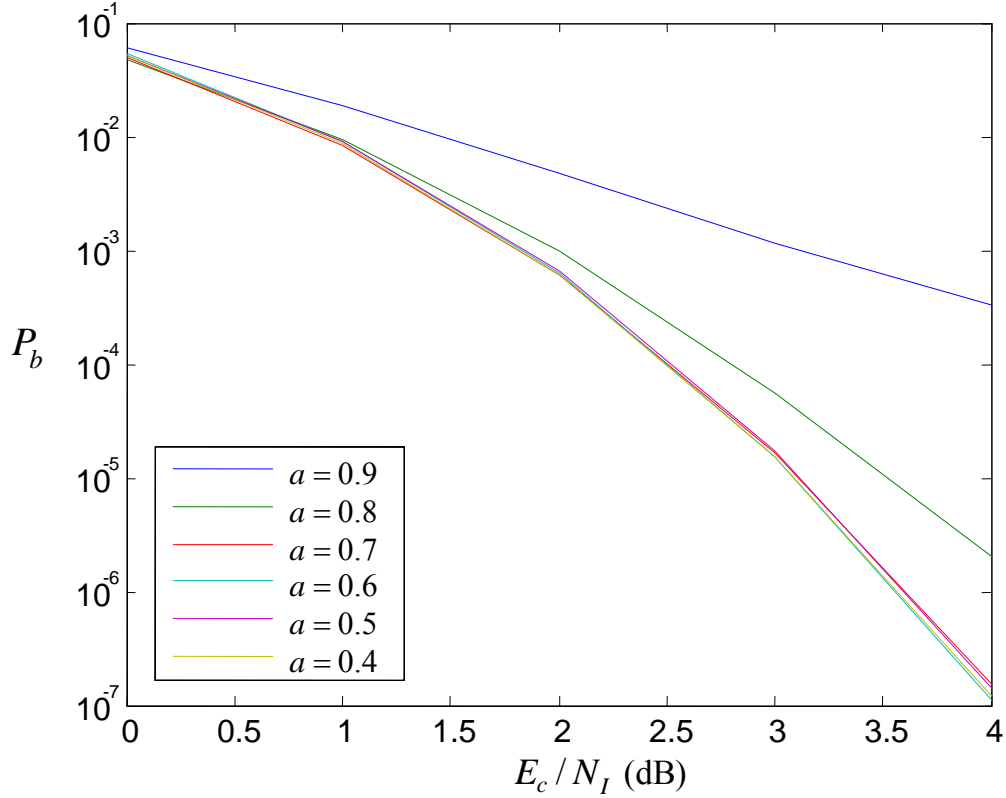


Figure 17. Performance of 32-BOK with (31,15) RS coding and EED for the double-pulse structure with  $\rho = 0.5$  and  $E_c/N_0 = 15$  dB for different values of  $a$ .

In Figure 18, we see the performance of 32-BOK with (31,15) RS coding, EED, and a diversity of two for  $a = 0.6$  for different values of  $\rho$  ( $E_c/N_0 = 2.5$  dB). At  $P_b = 10^{-5}$ , there is about 1.3 dB difference in  $E_c/N_I$  between the best and the worst performance, with the best performance when  $\rho = 1$  ( $E_c/N_I = 9.9$  dB) and the worst performance when  $\rho = 0.1$  ( $E_c/N_I = 11.2$  dB). The difference in performance is more obvious as  $E_c/N_0$  increases. This can be seen from Figure 19 for which  $E_c/N_0 = 15$  dB. At  $P_b = 10^{-5}$ , the difference between the best performance, for which  $\rho = 1$  ( $E_c/N_I = 2.1$  dB), and worst performance, for which  $\rho = 0.1$  ( $E_c/N_I = 5.9$  dB), is 3.8 dB.

From Figure 18 and Figure 19, while there is an improvement in absolute performance for the larger  $E_b/N_0$ , there is also a significant increase in the relative performance gap between  $\rho = 1$  and  $\rho = 0.1$ .

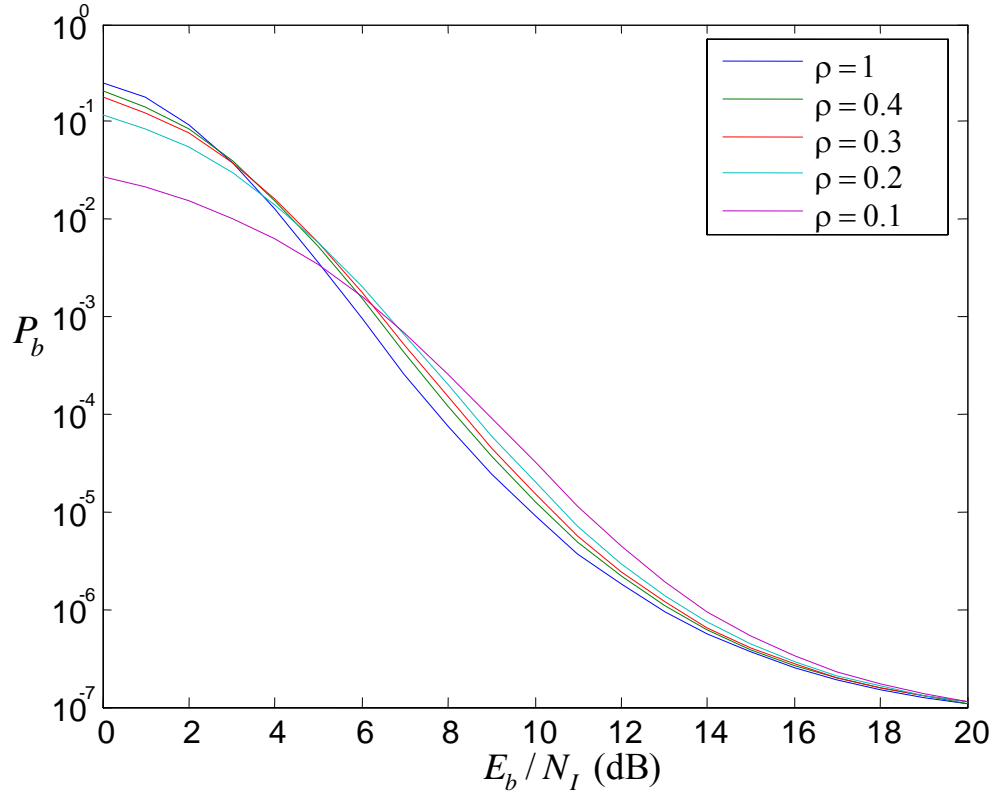


Figure 18. Performance of 32-BOK with (31,15) RS coding and EED ( $E_b/N_0 = 2.5$  dB,  $a = 0.6$ ) for the double-pulse structure.

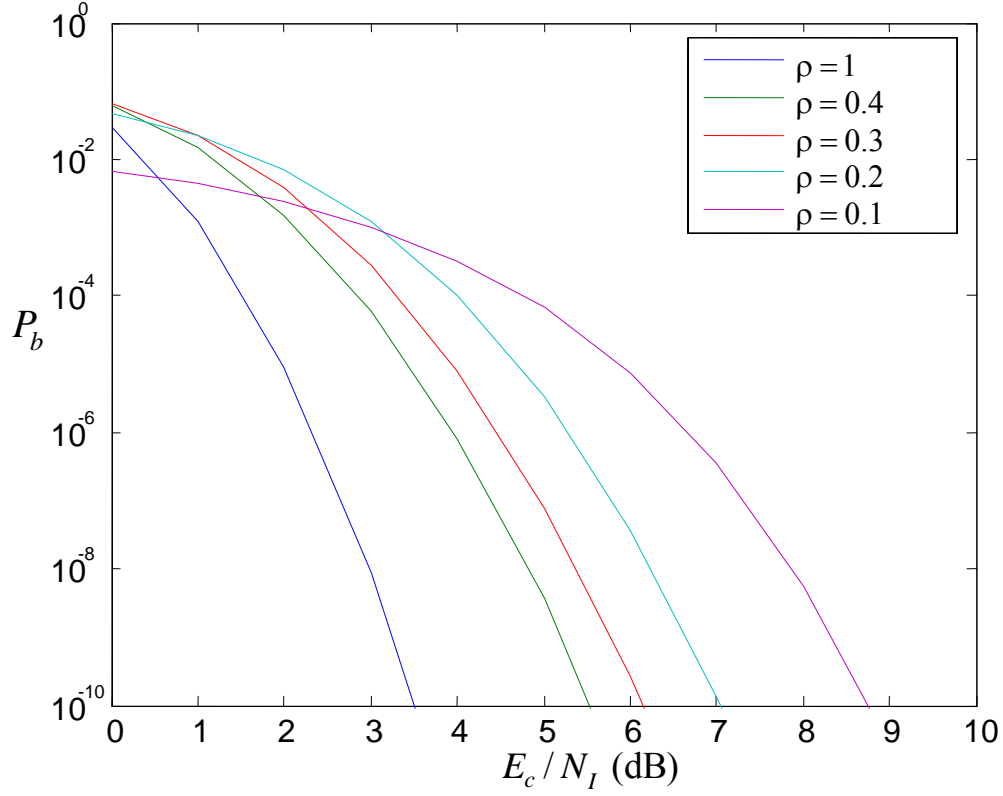


Figure 19. Performance of 32-BOK with (31,15) RS coding and EED ( $E_b/N_0 = 15$  dB,  $a = 0.6$ ) for the double-pulse structure.

In Figure 20, we compare the performance for 32-BOK with (31,15) RS coding and EED, both with and without diversity, for the case of an asymptotic convergence to  $10^{-7}$ . As expected, at  $P_b = 10^{-5}$ , we see that there is about 3 dB difference in performance between the two curves. This 3 dB improvement is due to the double-pulse advantage.

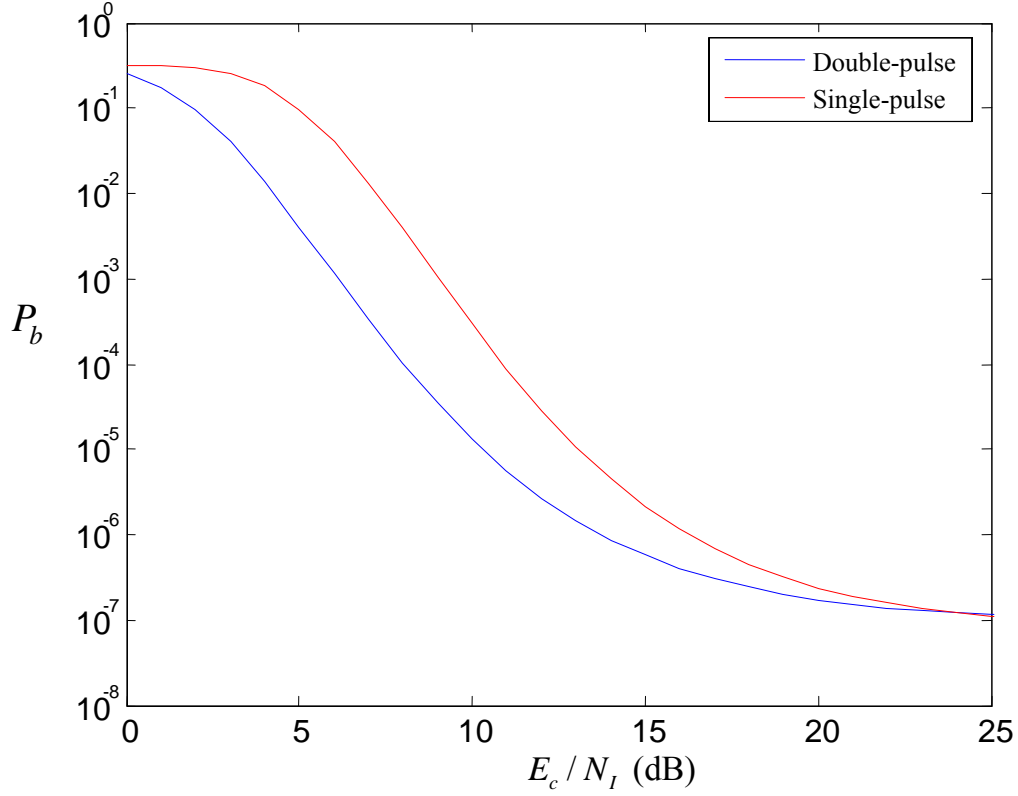


Figure 20. Performance of 32-BOK with (31,15) RS coding, EED,  $a = 0.6$ , for  $\rho = 1$  for the double-pulse ( $E_c / N_0 = 2.5$  dB) and the single-pulse structure ( $E_c / N_0 = 5.5$  dB).

The performance of 32-BOK with (31,15) RS coding both with and without EED for  $E_c / N_I = 2.5$  and 15 dB are shown in Figure 21 and Figure 22, respectively. In Figure 21, at  $P_b = 10^{-5}$ , for each  $\rho$ , the difference in performance between errors-only decoding and EED is less than 0.5 dB. In Figure 22, with  $E_c / N_0$  increased to 15 dB, we observe no difference in performance between EED and errors-only decoding. There is no benefit to EED as compared to errors-only decoding for the double-pulse structure (which is also the case for the single-pulse structure).

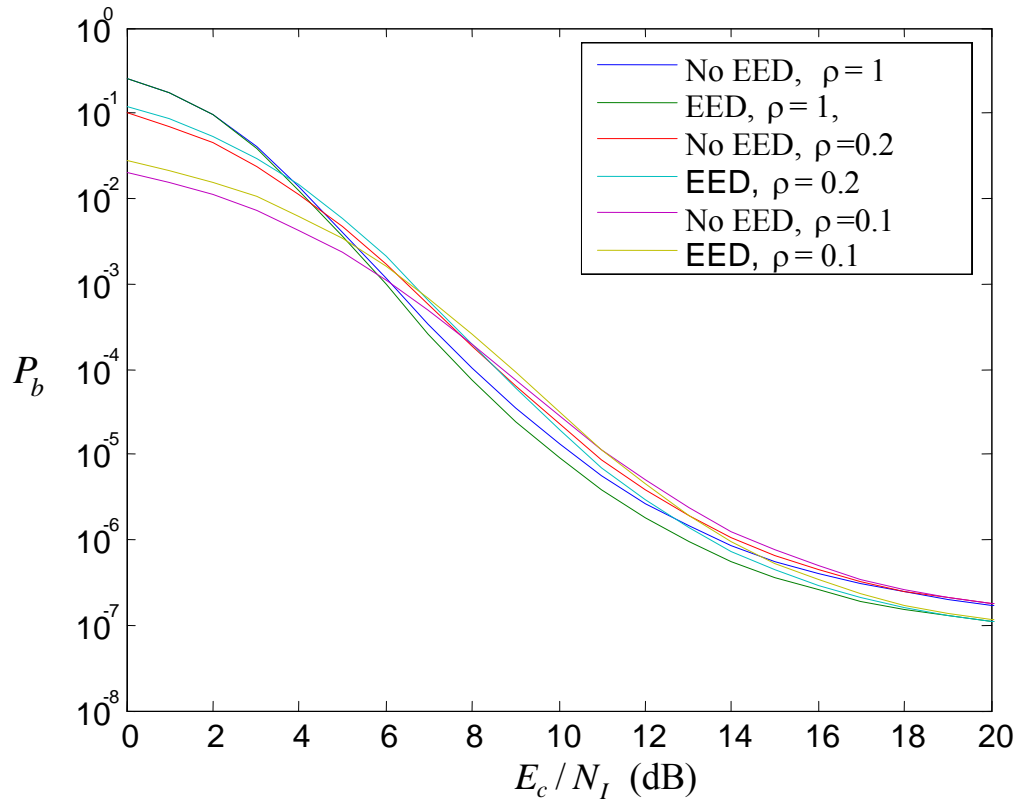


Figure 21. Performance of 32-BOK with (31,15) RS coding with and without EED with  $E_c/N_0 = 2.5$  dB and  $a = 0.6$  for different values of  $\rho$ .



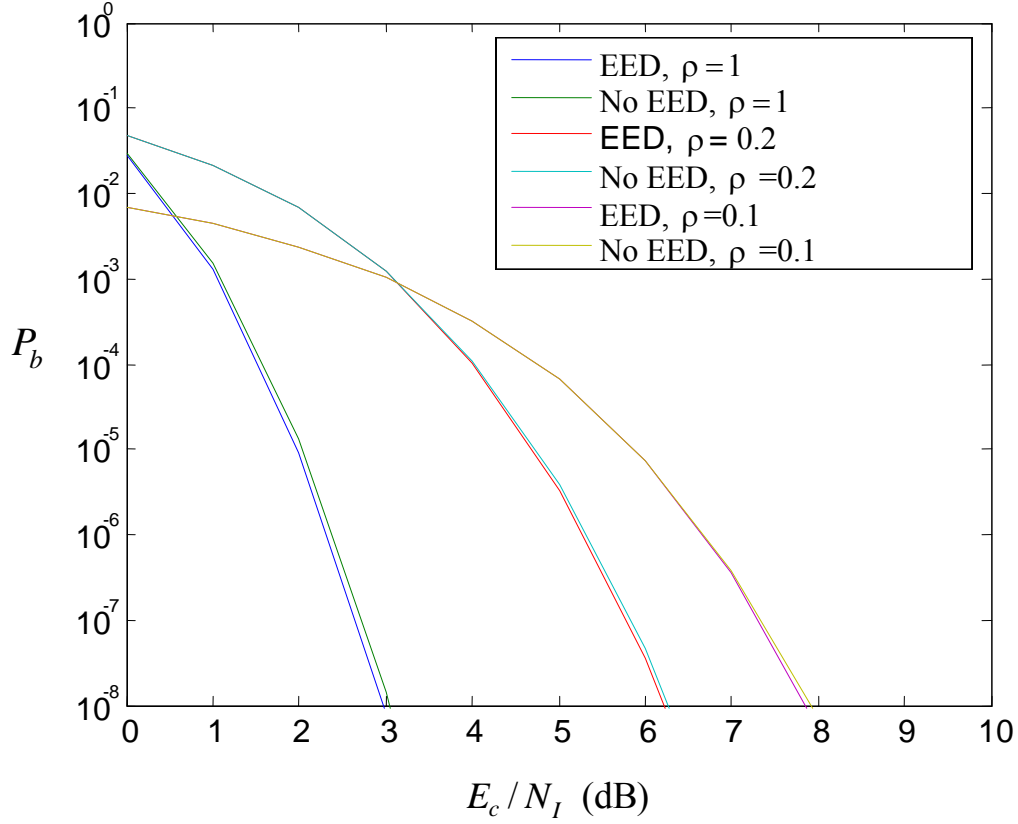


Figure 22. Performance of 32-BOK with (31,15) RS coding with and without EED with  $E_c/N_0 = 15$  dB and  $a = 0.6$  for different values of  $\rho$ .

#### D. PERFORMANCE WITH PERFECT-SIDE INFORMATION IN AWGN AND PNI

We have the conditional probability of channel chip error in (4.15) and the probability of channel symbol error with no diversity in (2.5). When only one diversity reception is affected by PNI, the decoding decision is based on the diversity reception that is free from PNI. From (2.5), (4.15) and (2.11), the probability of channel symbol error with a diversity of two is

$$P_s = (1-\rho)^2 p_s(0) + \rho^2 p_s(2) + 2\rho p_s(1) \quad (4.29)$$

where  $p_s(0)$  is the conditional probability of channel symbol error when PNI is not present in either diversity reception and is expressed as

$$p_s(0) = 1 - \frac{1}{\sqrt{2\pi}} \int_{-\sqrt{\frac{4rmE_c}{N_0}}}^{\infty} e^{-\frac{u^2}{2}} \left[ 1 - 2Q\left(u + \sqrt{\frac{4rmE_c}{N_0}}\right) \right]^{\frac{M}{2}-1} du. \quad (4.30)$$

The conditional probability of channel symbol error when only one of the diversity receptions suffers PNI (and is discarded) is

$$p_s(1) = 1 - \frac{1}{\sqrt{2\pi}} \int_{-\sqrt{2rmE_c/N_0}}^{\infty} e^{-\frac{u^2}{2}} \left[ 1 - 2Q\left(u + \sqrt{\frac{2rmE_c}{N_0}}\right) \right]^{\frac{M}{2}-1} du \quad (4.31)$$

Finally, the conditional probability of channel symbol error when both diversity receptions suffer PNI is given by

$$p_s(2) = 1 - \frac{1}{\sqrt{2\pi}} \int_{-\sqrt{\frac{2rm}{\rho \left( \frac{2}{\gamma_I}^{-1} + 2\gamma_c^{-1} \right)}}}^{\infty} e^{-\frac{u^2}{2}} \left[ 1 - 2Q\left(u + 2\sqrt{\frac{2rm}{\frac{2}{\gamma_I}^{-1} + 2\gamma_c^{-1}}}}\right) \right]^{\frac{M}{2}-1} du \quad (4.32)$$

The performance of 32-BOK with (31,15) RS coding with and without PSI is shown in Figure 23. When  $\rho = 1$ , as expected, there is no difference in performance whether PSI is used or not, which makes sense since the channel is experiencing barrage noise jamming. For  $P_b = 10^{-6}$ ,  $\rho = 0.2$ ,  $E_c/N_I = 6.7$  dB and  $E_c/N_I = 13.2$  dB is required for the waveform with and without PSI decoding, respectively. Thus, there is a gain of 6.5 dB with PSI. This is a significant improvement in performance. There is no benefit to PSI when  $\rho = 1$ , which corresponds to barrage noise jamming. Hence, PSI forces a jammer to adapt a barrage jamming strategy.

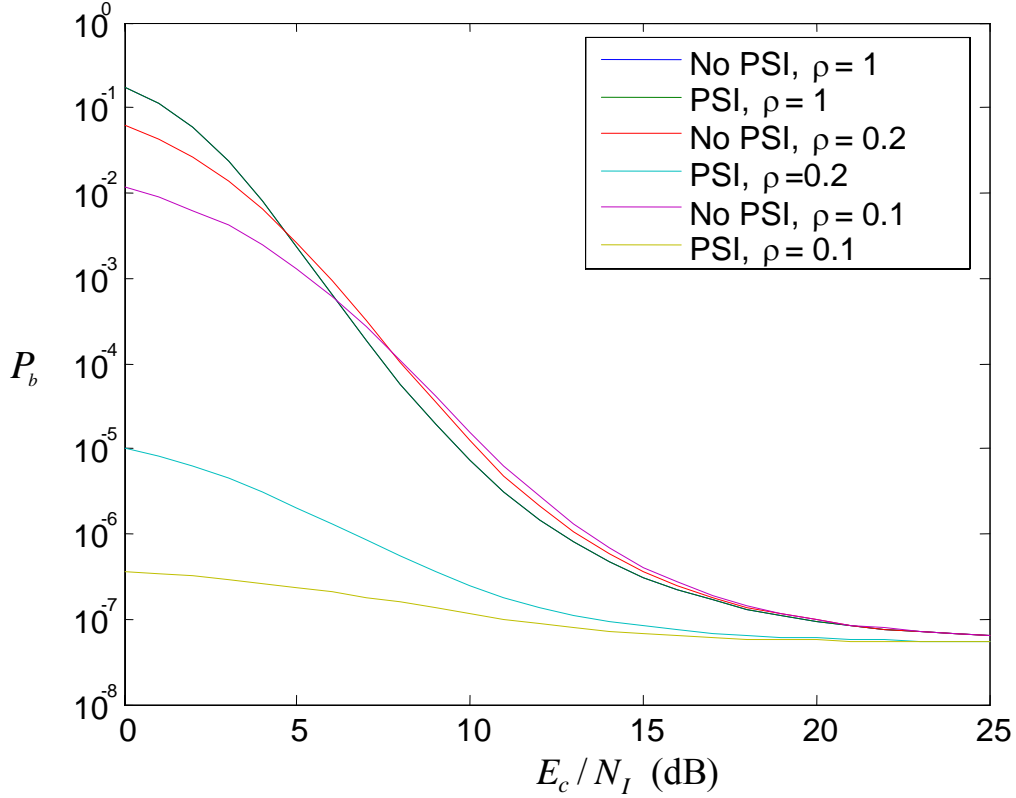


Figure 23. Performance for 32-BOK with (31,15) RS coding with and without PSI for different  $\rho$  ( $E_c/N_0 = 2.5$  dB).

## E. CHAPTER SUMMARY

In this chapter, the performance of the alternative JTIDS/Link-16 waveform with a diversity of two (double-pulse structure) was investigated both with and without EED and for AWGN only as well as AWGN plus PNI. We saw that the waveform performs better when  $\rho=1$  (barrage noise interference) than  $\rho<1$ . We also see that EED decoding does not substantially improve performance for the receiver when both AWGN and PNI are present. We also analyzed the performance of the waveform with PSI, and the results show a significant improvement in performance for a channel with AWGN with PNI. In Chapter V, we compare the performance of the alternative JTIDS/Link-16 waveform and the JTIDS/Link-16 waveform for different channels and pulse structures.

THIS PAGE INTENTIONALLY LEFT BLANK

## **V. COMPARISON OF THE JTIDS/LINK-16 WAVEFORM AND THE ALTERNATIVE JTIDS/LINK-16 WAVEFORM**

In Chapter IV, we analyzed the performance of 32-BOK with (31,15) RS coding waveform, herein known as the alternative JTIDS/Link-16 waveform, using a double-pulse structure. We considered errors-only decoding as well as EED. In this chapter, we compare the performance of the alternative JTIDS/Link-16 waveform with the original JTIDS/Link-16 waveform. Detailed analysis of JTIDS can be found in [7]. Results from [7] are used to obtain the performance of the original JTIDS/Link-16 waveform, which is compared to the proposed alternative JTIDS/Link-16 waveform.

### **A. COMPARISON OF JTIDS/LINK-16 AND THE ALTERNATIVE JTIDS/LINK-16 WAVEFORM, SINGLE-PULSE STRUCTURE**

In this section, we compare the performance of the alternative JTIDS/Link-16 waveform with the existing JTIDS/Link-16 waveform for the single-pulse structure. Both AWGN and AWGN with PNI are considered. In addition, we also compare the performance when both waveforms use EED. The performance of the alternative waveform with PSI compared to JTIDS/Link-16 waveform with EED is also shown.

#### **1. Comparison for AWGN**

The probability of information bit error for both the alternative JTIDS/Link-16 waveform and the JTIDS/Link-16 waveform in AWGN is shown in Figure 24. At  $P_b = 10^{-3}$ ,  $E_b / N_0 = 3.8$  dB and  $E_b / N_0 = 6.1$  dB for the alternative JTIDS/Link-16 waveform and JTIDS/Link-16 waveform, respectively. This yields a 2.3 dB gain for the proposed waveform over the JTIDS/Link-16 waveform in AWGN. Similarly, at  $P_b = 10^{-5}$ , there is a 2.3 dB gain for the alternative JTIDS/Link-16 waveform over the JTIDS/Link-16 waveform, with  $E_b / N_0 = 4.7$  dB and  $E_b / N_0 = 7.0$  dB required for the alternative waveform and the JTIDS/Link-16 waveform, respectively.

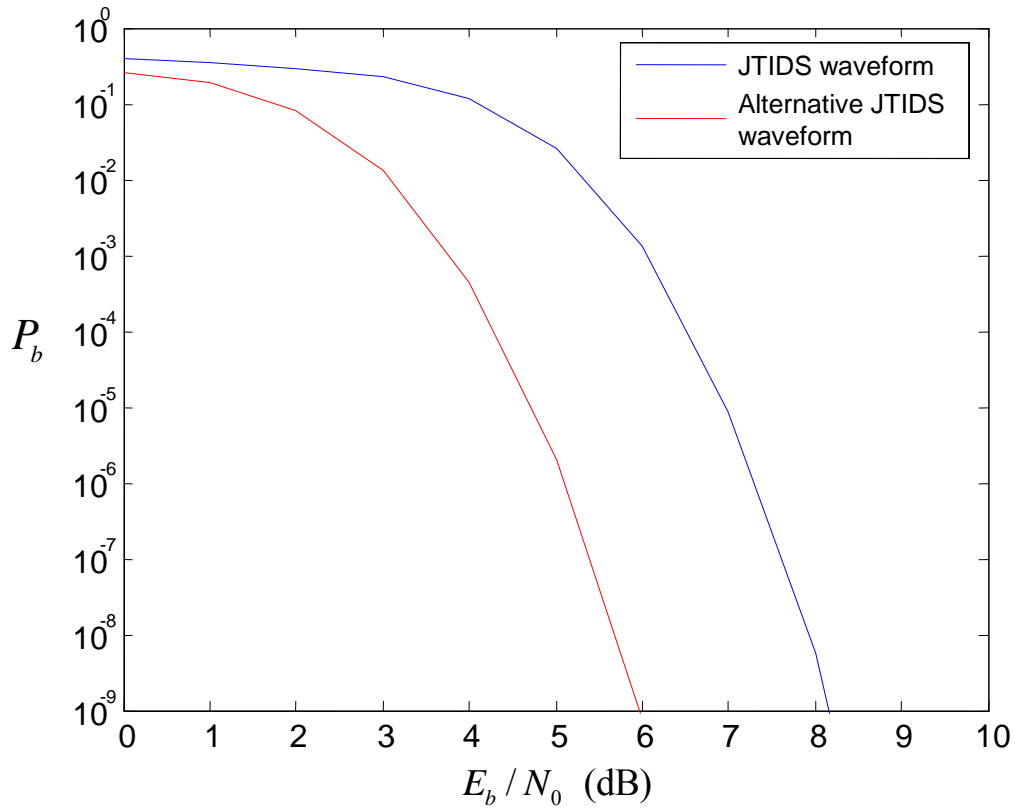


Figure 24. Performance of 32-BOK with (31,15) RS coding and JTIDS/Link-16 in AWGN.

## 2. Comparison in AWGN and PNI

The probability of information bit error for the JTIDS/Link-16 and the alternative JTIDS/Link-16 waveform in AWGN and PNI is shown in Figure 25 for different values of  $\rho$ . For the plots to approach  $10^{-7}$ , the  $E_b/N_0$  required for the alternative waveform is 5.5 dB, while the  $E_b/N_0$  required for the JTIDS waveform is 7.6 dB. This gives a difference of 2.1 dB for both curves to approach  $P_b = 10^{-7}$  at  $E_b/N_0 = 25$  dB.

At  $P_b = 10^{-5}$ ,  $\rho = 1$ , the difference in  $E_b/N_I$  between the alternative JTIDS/Link-16 waveform ( $E_b/N_I = 12.7$  dB) and the JTIDS/Link-16 waveform ( $E_b/N_I = 15.1$  dB) is

2.4 dB. Similarly, for  $\rho = 0.2$  and  $0.1$ , the difference in  $E_b / N_I$  between the alternative JTIDS/Link-16 waveform ( $E_b / N_I = 13.5$  dB) and the JTIDS waveform ( $E_b / N_I = 16.2$  dB) is about 2.7 dB.

From the above, we see that the alternative JTIDS/Link-16 waveform performs better than the JTIDS/Link-16 waveform with an improvement of about 2.4 dB to 2.7 dB at  $P_b = 10^{-5}$  when both waveform converge to  $P_b = 10^{-7}$  at  $E_b / N_I = 25$  dB for the single-pulse structure. Clearly, the JTIDS/Link-16 waveform would have a substantially inferior performance if the two waveforms were compared on an equal  $E_b / N_0$  basis.

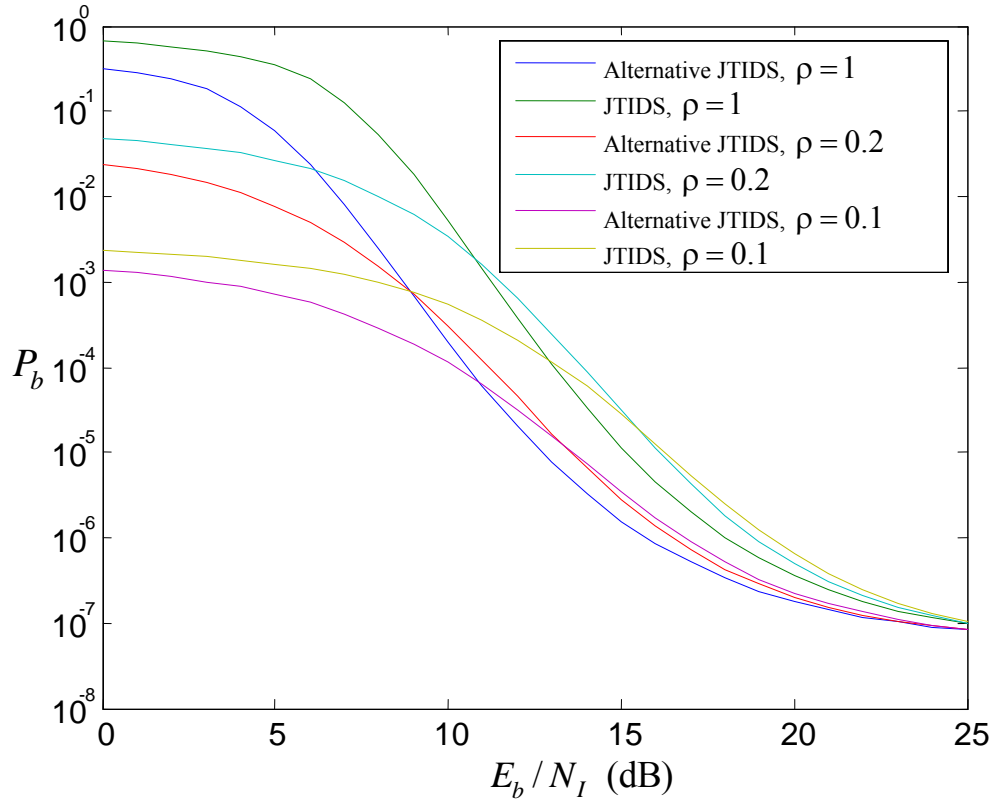


Figure 25. Performance of 32-BOK with (31,15) RS coding ( $E_b / N_0 = 5.5$  dB) and JTIDS waveform ( $E_b / N_0 = 7.6$  dB) for different values of  $\rho$ .

### 3. Performance Using EED in AWGN and PNI

The performance of the alternative JTIDS/Link-16 waveform ( $a=0.6$ ,  $E_b/N_0=5.5$  dB) and the JTIDS/Link-16 waveform (threshold=14,  $E_b/N_0=7.3$  dB) is compared in Figure 26, which plots convergence to  $P_b = 10^{-7}$  at  $E_b/N_I = 25$  dB. For the alternative JTIDS/Link-16 waveform to converge to  $P_b = 10^{-7}$ ,  $E_b/N_0 = 5.5$  dB is required as compared to  $E_b/N_0 = 7.3$  dB for the JTIDS/Link-16 waveform for a difference of 1.8 dB.

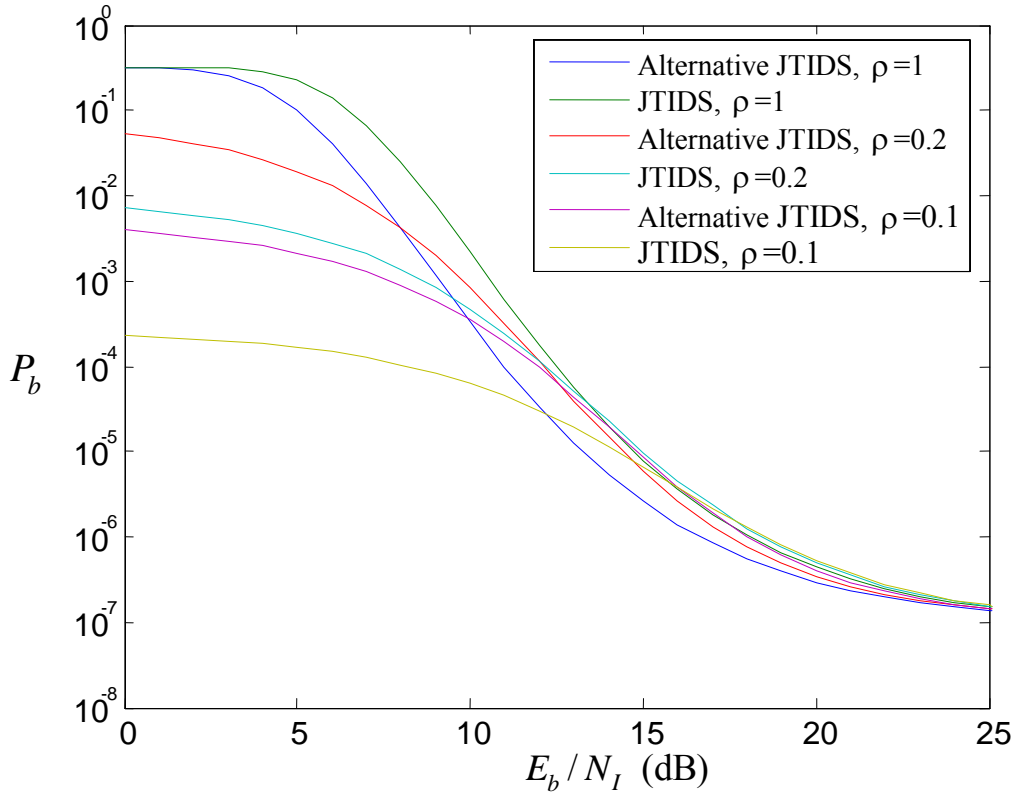


Figure 26. Performance of the alternative JTIDS/LINK-16 waveform ( $a=0.6$ ,  $E_b/N_0=5.5$  dB) and the JTIDS/Link-16 waveform with EED (threshold=14,  $E_b/N_0=7.3$  dB) for different values of  $\rho$ .

For  $\rho=1$ , we see that the alternative waveform is superior to the JTIDS/Link-16 waveform for all values of  $E_b/N_I$  until they converge at  $P_b = 10^{-7}$ . There is a gain of 1.5



dB using the alternative JTIDS/Link-16 waveform for  $\rho=1$  at  $P_b = 10^{-5}$ . For  $\rho = 0.2$ , the JTIDS/Link-16 waveform performs better than the alternative waveform for  $E_b / N_I < 12.5$  dB. For  $\rho=0.1$ , the JTIDS/Link-16 waveform performs better than the alternative JTIDS/Link-16 waveform for  $E_b / N_I < 16.5$  dB. The alternative JTIDS/Link-16 waveform performs better than the existing JTIDS/Link-16 waveform for larger  $\rho$  and increasing  $E_b / N_I$ . Another conclusion is that, while EED was shown in a previous section not to improve performance for the alternative waveform, this is not the case for the existing JTIDS/Link-16 waveform.

We examine both the alternative waveform and the JTIDS/Link-16 waveform when  $E_b / N_0 = 7.3$  dB for  $\rho=1$  and 0.5 in Figure 27. At  $P_b = 10^{-5}$ , the alternative waveform is superior to the JTIDS/Link-16 waveform with a gain of 6.5 dB and 5.5 dB for  $\rho = 1$  and 0.5, respectively. The alternative waveform performs much better than the existing JTIDS/Link-16 waveform when  $E_b / N_0$  is the same for both.

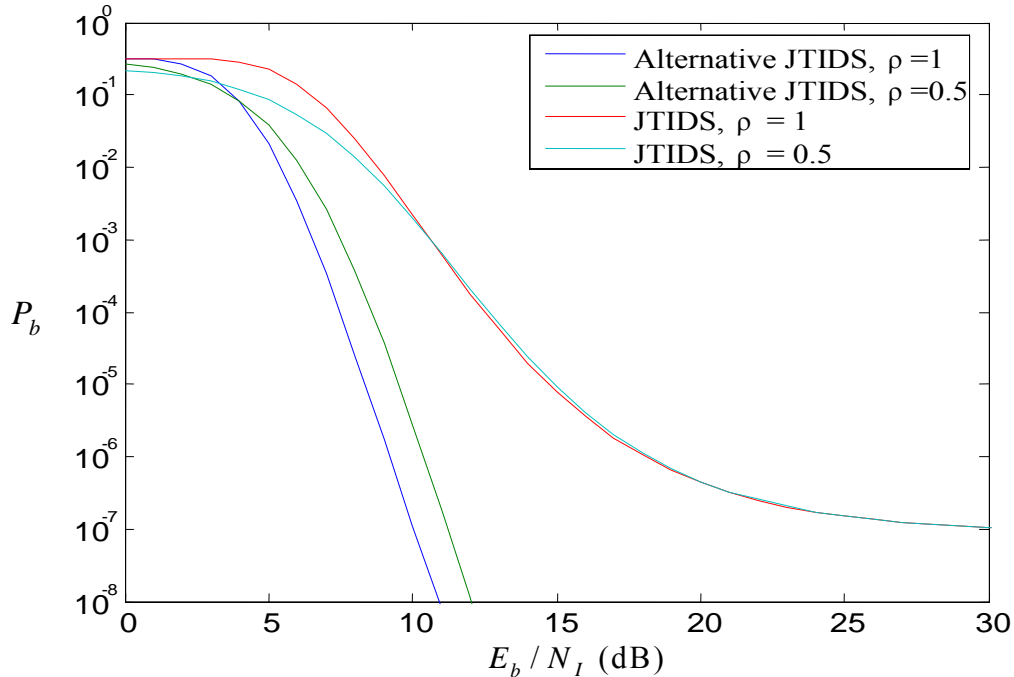


Figure 27. Performance of the alternative JTIDS/Link-16 waveform ( $a = 0.6$ ) and the JTIDS/Link-16 waveform (threshold=14) with EED at  $E_b / N_0 = 7.3$  dB for  $\rho=1$  and 0.5.

## **B. COMPARSION OF THE JTIDS/LINK-16 AND THE ALTERNATIVE JTIDS/LINK-16 WAVEFROM, DOUBLE-PULSE STRUCTURE**

In this section, we compare the performance between the alternative JTIDS/Link-16 waveform and the original JTIDS/Link-16 waveform for the double-pulse structure. The analyses consider both AWGN only and AWGN plus PNI. In addition, we compare performance when both waveforms use EED.

### **1. Comparison in AWGN**

The probability of information bit error for the alternative JTIDS/Link-16 waveform and the JTIDS/Link-16 waveform in AWGN for the double-pulse structure is shown in Figure 28. At  $P_b = 10^{-5}$ ,  $E_c / N_0 = 1.7$  dB and  $E_c / N_0 = 4$  dB for the alternative JTIDS/Link-16 waveform and the existing JTIDS/Link-16 waveform, respectively. This gives a 2.3 dB gain for the proposed JTIDS/Link-16 waveform as compared to the JTIDS/Link-16 waveform.

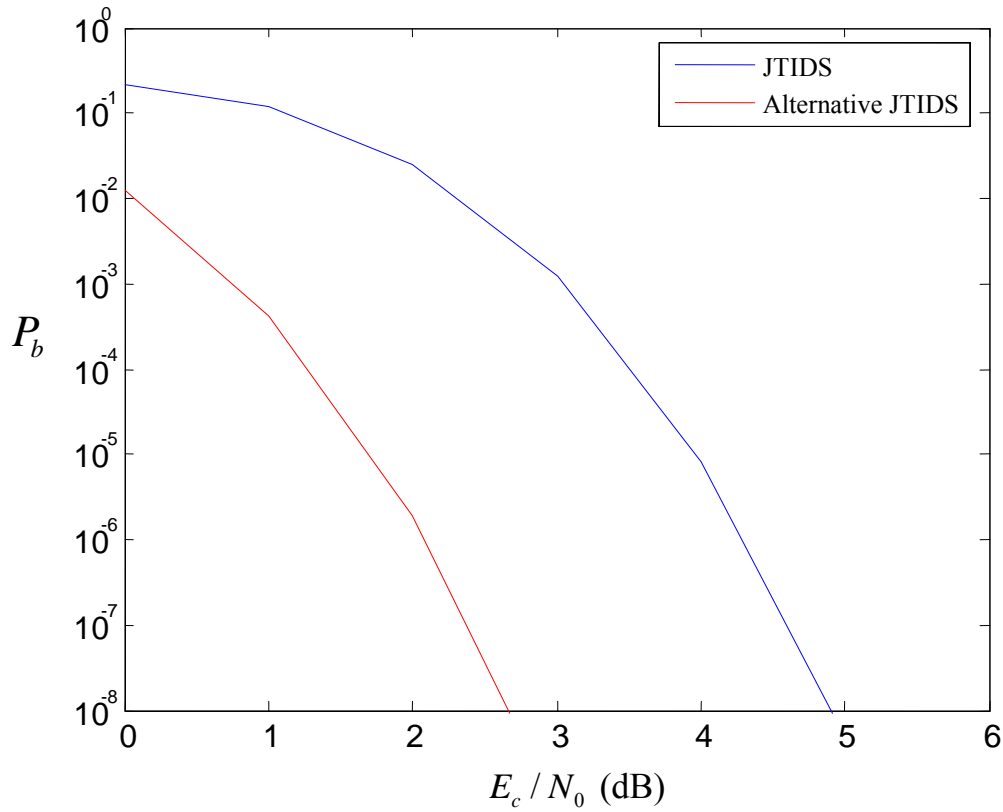


Figure 28. Performance of the alternative JTIDS/Link-16 waveform and the JTIDS waveform for the double-pulse structure.

From Figure 24, for the single-pulse structure and  $P_b = 10^{-5}$ , the alternative JTIDS/Link-16 waveform requires  $E_b / N_0 = 4.7$  dB. As a result, there is only a 0.7 dB advantage of the double-pulse JTIDS/Link-16 waveform over the single-pulse alternative JTIDS/Link-16 waveform.

## 2. Performance Comparison in AWGN and PNI

The probability of bit error for the JTIDS/Link-16 and the alternative JTIDS/Link-16 waveform for the double-pulse structure in both AWGN and PNI is shown in Figure 29. We consider the case where the performance converges to  $10^{-7}$  for  $\rho = 1, 0.2$  and  $0.1$ . For the graph to approach  $P_b = 10^{-7}$ , the alternative waveform requires

$E_c / N_0 = 2.4$  dB, while the JTIDS/Link-16 waveform requires  $E_c / N_0 = 4.5$  dB. This gives a 2.1 dB gain for the alternative JTIDS/Link-16 waveform as compared to the JTIDS/Link-16 waveform.

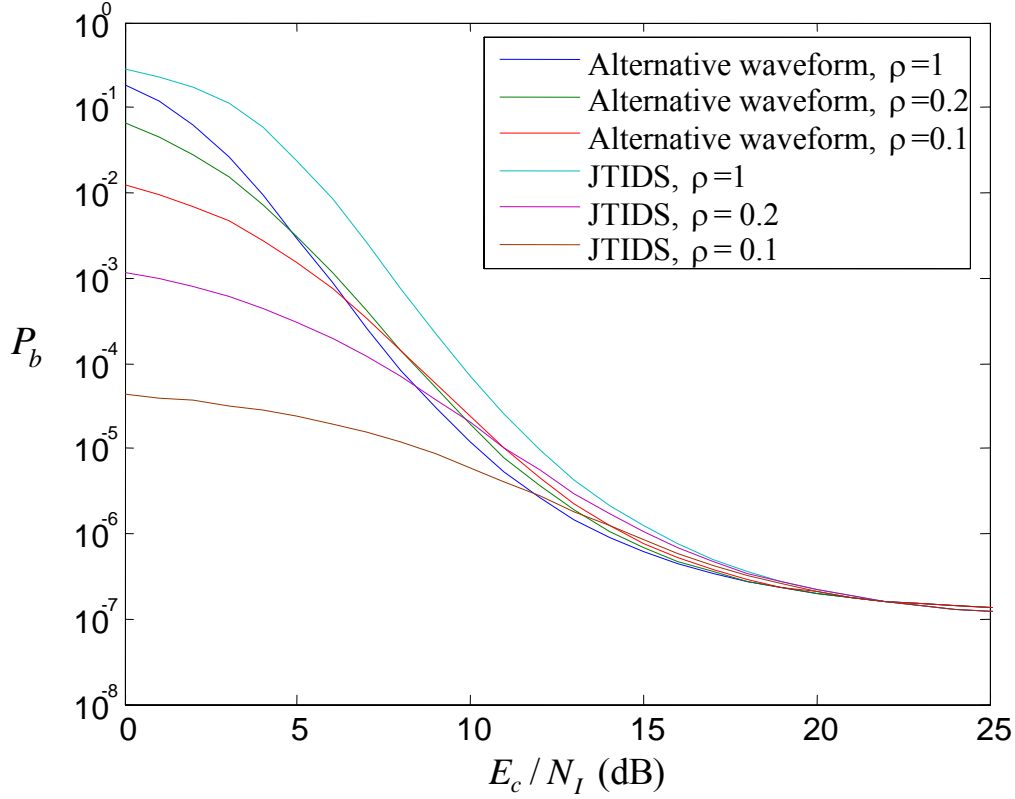


Figure 29. Performance of the alternative JTIDS/Link-16 waveform ( $E_c / N_0 = 2.4$  dB) and the JTIDS/Link-16 waveform ( $E_c / N_0 = 4.5$  dB) for the double-pulse structure.

At  $P_b = 10^{-5}$ ,  $\rho = 1$ , the difference in  $E_c / N_I$  between the alternative JTIDS/Link-16 waveform ( $E_c / N_I = 10.2$  dB) and the JTIDS/Link-16 waveform ( $E_c / N_I = 12$  dB) is 1.8 dB, while for  $\rho = 0.1$ , the JTIDS/Link-16 waveform has a gain of 2.4 dB over the alternative waveform. For  $E_c / N_I > 17$  dB, there is no difference in performance between the waveforms. For  $\rho = 0.2$ , when  $E_c / N_I < 11$  dB, the JTIDS/Link-16 waveform performs better than the alternative waveform, and we see no significant difference in performance between the two waveforms for  $E_c / N_I > 11$  dB.

### 3. Performance with EED in AWGN and PNI

The performance of the alternative JTIDS/Link-16 waveform ( $a = 0.6$ ,  $E_c / N_0 = 2.5$  dB) and the JTIDS/Link-16 waveform (threshold = 14,  $E_c / N_0 = 4.4$  dB) for the double-pulse structure, where the results all converge to  $P_b = 10^{-7}$ , are shown in Figure 30. For the alternative JTIDS/Link-16 waveform to converge to  $P_b = 10^{-7}$ ,  $E_c / N_0 = 2.5$  dB is required as compared to  $E_c / N_0 = 4.4$  dB for the JTIDS/Link-16 waveform. The difference is 1.9 dB. At  $P_b = 10^{-6}$  dB, the difference in gain between the alternative JTIDS waveform and the JTIDS/Link-16 waveform is less than 1 dB.

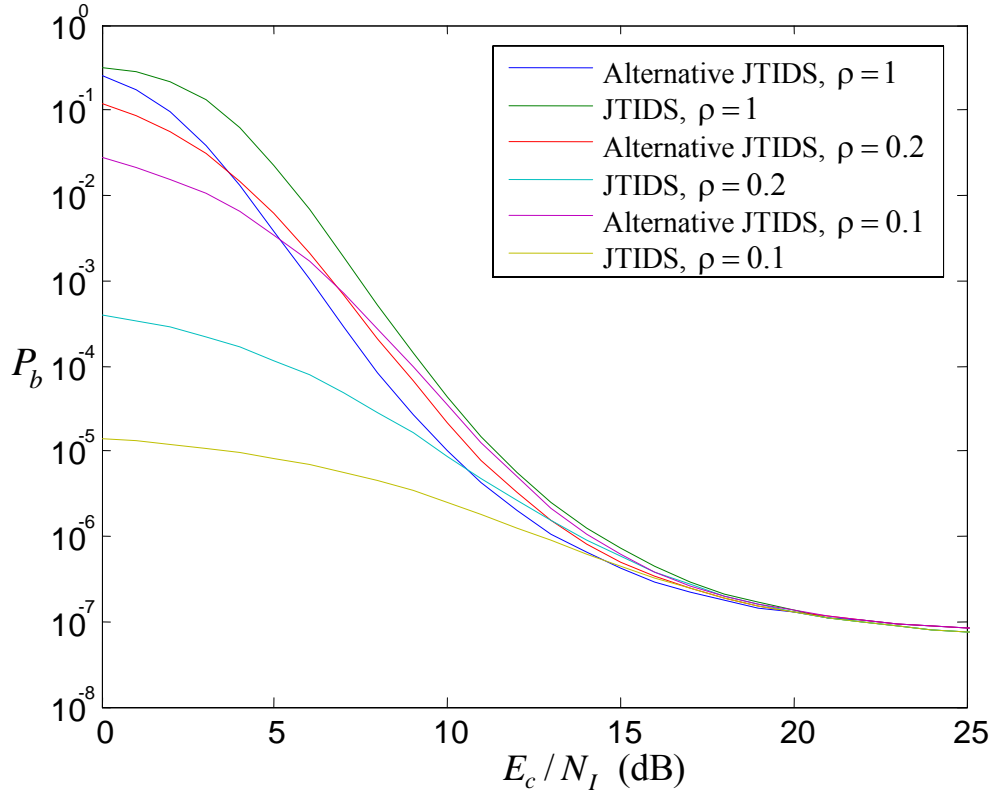


Figure 30. Performance of the alternative JTIDS/LINK-16 waveform ( $a=0.6$ ,  $E_c / N_0=2.5$  dB) and the JTIDS/Link-16 waveform (threshold=14,  $E_c / N_0=4.4$  dB) with EED.

The alternative JTIDS/Link-16 waveform consistently outperforms the JTIDS/Link-16 waveform for all values of  $E_c / N_I$  for  $\rho=1$  until the results converge at  $P_b=10^{-7}$ . There is a difference of 1.4 dB between the performance of the two waveforms at  $P_b=10^{-5}$  for  $\rho=1$ . However, for  $\rho=0.2$  and  $0.1$ , the JTIDS/Link-16 waveform outperform the alternative waveform. This is because EED does not provide an improvement in performance for 32-BOK with RS coding (as shown in Chapter III and IV for the single-pulse and the double-pulse structure, respectively), while there is improvement in performance for the JTIDS/Link-16 waveform with EED [7].

In Figure 31, the case for the alternative waveform and the JTIDS/Link-16 waveform, both with  $E_c / N_0 = 4.4$  dB for  $\rho=1$  and  $0.5$ , is examined. At  $P_b=10^{-5}$ , the alternative waveform is superior to the JTIDS/Link-16 waveform with a gain of 6.3 dB and 5.5 dB for  $\rho=1$  and  $0.5$ , respectively. The alternative waveform outperforms the existing JTIDS/Link-16 waveform when both have the same  $E_c / N_0$  regardless of  $E_b / N_I$ .

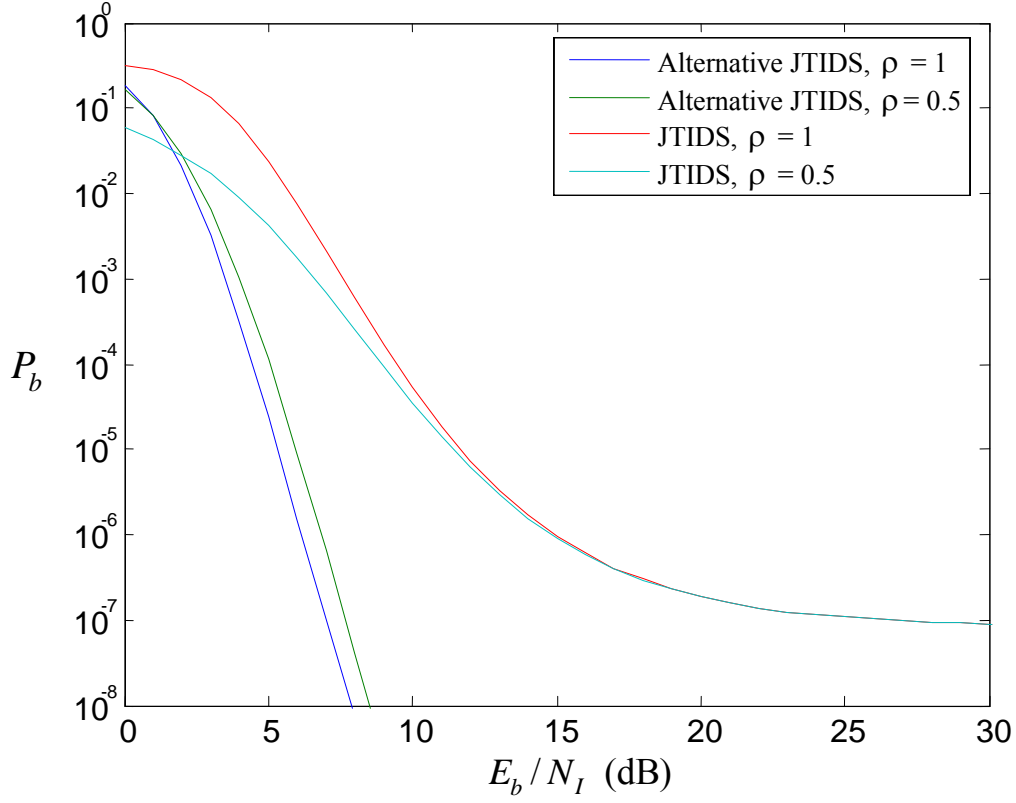


Figure 31. Performance of the alternative JTIDS/Link-16 waveform ( $a = 0.6$ ) and the JTIDS/Link-16 waveform (threshold=14) with EED at  $E_c/N_0 = 4.4$  dB.

#### 4. Performance with PSI in AWGN and PNI

The performance for the alternative JTIDS/Link-16 waveform with PSI is compared with that obtained for the JTIDS/Link-16 waveform with EED in Figure 32. We see that the alternative waveform with PSI performs better than the existing JTIDS/Link-16 waveform for all values of  $\rho$ . At  $P_b = 10^{-5}$ ,  $\rho = 0.2$  and 1, there is an improvement of 5.8 dB and 1.4 dB, respectively, for the alternative JTIDS/Link-16 waveform over the JTIDS/Link-16 waveform. The improvement is only 1.4 dB for  $\rho = 1$  but 5.8 dB for  $\rho = 0.2$  since there is no benefit to PSI when  $\rho = 1$ .

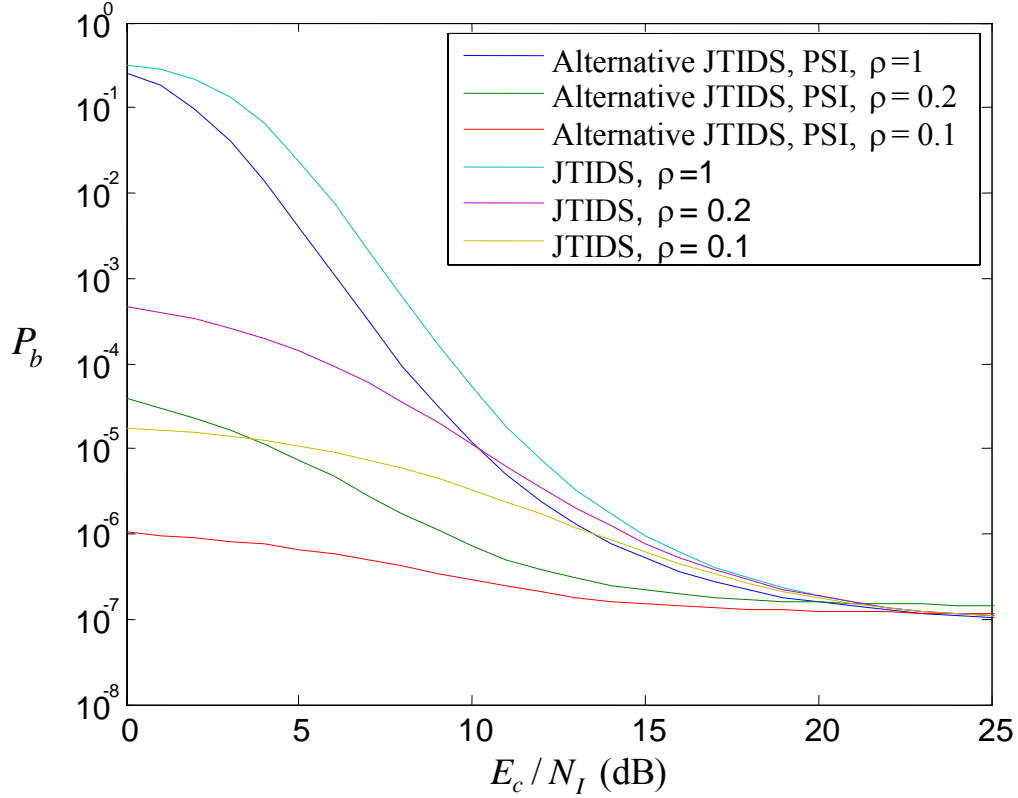


Figure 32. Performance for the alternative JTIDS/Link-16 (PSI,  $E_c / N_0 = 2.5$  dB) and the JTIDS/Link-16 waveform (EED, threshold=14,  $E_c / N_0 = 4.3$  dB).

### C. CHAPTER SUMMARY

In this chapter, we compared the performance of the alternative JTIDS/Link-16 waveform and the JTIDS/Link-16 waveform for a channel with AWGN as well as PNI and with different pulse structures (single-pulse and double-pulse structure). In addition, we compared the performance of the alternative waveform with PSI in an AWGN plus PNI environment. The result shows a significant improvement over the JTIDS/Link-16 waveform for  $\rho < 1$ . In the next chapter, we summarize the findings of this thesis.



## VI. CONCLUSIONS AND FUTURE RESEARCH AREAS

### A. CONCLUSIONS

This thesis presents an alternative JTIDS/Link-16 waveform, 32-BOK with (31,15) RS coding, to the JTIDS/Link-16 waveform. We first analyzed the performance of the proposed waveform and subsequently compared its performance with the existing JTIDS/Link-16 waveform for both errors-and-erasure and errors-only decoding, with and without diversity, both in AWGN as well as PNI channel. In addition, we also considered the efficacy of PSI.

Based on the results obtained, we see that 32-BOK with (31,15) RS coding performs better than the existing JTIDS waveform in AWGN. In an AWGN plus PNI channel, the alternative waveform outperforms the JTIDS/Link-16 in barrage noise interference ( $\rho = 1$ ) both with and without EED. When the channel has PNI and  $\rho < 1$ , using EED and with both waveforms asymptotically approaching  $P_b = 10^{-7}$  for large  $E_b / N_t$ , the alternative waveform does not outperform the JTIDS/Link-16 waveform; however, this is at the expense of the JTIDS/Link-16 waveform requiring a higher  $E_c / N_0$  than the alternative JTIDS/Link-16 waveform. When the waveforms both have the same  $E_c / N_0$ , the alternative JTIDS/Link-16 clearly outperforms the JTIDS/Link-16 waveform by more than 5 dB for both single-pulse and double-pulse structures (at  $P_b = 10^{-5}$ ).

We also found no benefit to EED for the alternative waveform since there is virtually no improvement in performance as compared to errors-only decoding. This result is rather surprising since EED usually improves the performance of a waveform when PNI is present. We have also shown that PSI provides a significant improvement in performance in an AWGN plus PNI environment.

## **B. FUTURE RESEARCH AREAS**

We have examined an alternative JTIDS/Link-16 waveform that consists of 32-BOK with (31,15) RS coding and provides an improvement over the existing JTIDS/Link-16 waveform. One possible follow-on research area would be to analyze the alternative waveform for a fading channel. In addition, the performance for this waveform may be further improved using concatenated code. A possible candidate for a concatenated code is a RS code as the outer code and a non-binary convolutional code as the inner code. Finally, if 64-BOK is used, not only should performance improve while continuing to have 32 chips per channel symbol, but each symbol will now have a parity bit associated with it that may be able to be used to improve performance.

## LIST OF REFERENCES

- [1] Northrop Grumman Corporation, Information Technology Communication & Information Systems Division, *Understanding Link-16: A Guidebook for New Users*, NCTSI, San Diego, CA, Sept 2001 (Prepared, 1994, First Revision, 1998; Second Revision, 1998; Third Revision, 2001).
- [2] Dr Carlo Kopp, "Network Centric Warfare Fundamentals – Part 3" [Online]. Available: <http://www.ausairpower.net/NCW-101-3.pdf>.
- [3] John Asenstorfer, Thomas Cox and Darren Wilksh, *Tactical Data Link Systems and the Australian Defence Force (ADF) – Technology Developments and Interoperability Issues*, DSTO-TR-1470, pp 8-10, Feb 2004.
- [4] Michael B. Pursley, Thomas C. Royster and Michael Y. Tan, "High-Rate Direct-Sequence Spread Spectrum," *Proc. IEEE MILCOM*, vol. 2, pp. 1101-1106, Oct 2003.
- [5] Michael B. Pursley and Thomas C. Royster, "High-Rate Direct-Sequence Spread Spectrum With Error-Control Coding," *IEEE Transactions on Communications*, vol. 54, No.9, pp. 1693-1702, Sept 2006.
- [6] Hua Wang, Jingming Kuang, Zheng Wang, Hui Xu, "Transmission Performance Analysis of JTIDS," *Proc. IEEE MILCOM*, vol. 4, pp. 2264 – 2268, Oct 2005.
- [7] Chi-Han Kao, "Performance Analysis of JTIDS/Link-16-type Waveform Subject to Narrowband Waveform over Slow, Flat Nakagami Fading Channels," *Proc. IEEE MILCOM*, Nov 2008., submitted for publication.
- [8] B. Sklar, *Digital Communications: Fundamental and Applications*, 2<sup>nd</sup> Edition, Prentice Hall, Upper Saddle River, NJ, 2001.
- [9] Clark Robertson, Notes for EC4550 Digital Communications, Naval Postgraduate School, Monterey, CA, 2007.
- [10] Clark Robertson, Notes for EC4550 Sequential and Parallel Diversity, Naval Postgraduate School, Monterey, CA, 2007.
- [11] Clark Robertson, Notes for Frequency-Hopped Spread Spectrum, Naval Postgraduate School, Monterey, CA, 2007.
- [12] Clark Robertson, Notes for EC4580 Error Correction Coding; Discrete Memory Channel, Naval Postgraduate School, Monterey, CA, 2007.

- [13] Georgios Zouros and Clark Robertson, "Performance Analysis of BPSK with Errors and Erasures Decoding to Mitigate the Effects of Pulse-Noise Interference," *Proc. IEEE MILCOM*, Oct 2006.

## **INITIAL DISTRIBUTION LIST**

1. Defense Technical Information Center  
Ft. Belvoir, Virginia
2. Dudley Knox Library  
Naval Postgraduate School  
Monterey, California
3. Professor Jeffery B. Knorr, Chairman  
Department of Electrical and Computer Engineering  
Naval Postgraduate School  
Monterey, California
4. Professor R. Clark Robertson  
Department of Electrical and Computer Engineering  
Naval Postgraduate School  
Monterey, California
5. Professor Roberto Cristi  
Department of Electrical and Computer Engineering  
Naval Postgraduate School  
Monterey, California
6. Seah Peng Hwee  
Defence Science and Technology Agency  
Singapore
7. Cham Kok Kiang  
Defence Science and Technology Agency  
Singapore